Published in final edited form as:
J Neurosci. 2011 February 9; 31(6): 2035–2051. doi:10.1523/JNEUROSCI.5634-10.2011.

α-Synuclein Negatively Regulates PKCδ Expression to Suppress Apoptosis in Dopaminergic Neurons by Reducing p300 HAT Activity

Huajun Jin[1], **Arthi Kanthasamy**[1], **Anamitra Ghosh**[1], **Yongjie Yang**[2], **Vellareddy Anantharam**[1], and **Anumantha Kanthasamy**[1]

[1]Parkinson's Disorder Research Laboratory, Iowa Center for Advanced Neurotoxicology, Department of Biomedical Sciences, Iowa State University, Ames, IA 50011

[2]Department of Neurology and Neuroscience, Johns Hopkins University, Baltimore, MD 21287

Abstract

We recently demonstrated that PKCδ, an important member of the novel PKC family, is a key oxidative stress-sensitive kinase that can be activated by caspase-3-dependent proteolytic cleavage to induce dopaminergic neuronal cell death. We now report a novel association between α-synuclein (αsyn), a protein associated with the pathogenesis of Parkinson's diseases (PD), and PKCδ, in which αsyn negatively modulates the p300 and NFκB dependent transactivation to down-regulate proapoptotic kinase PKCδ expression and thereby protects against apoptosis in dopaminergic neuronal cells. Stable-expression human wild-type αsyn at physiological levels in dopaminergic neuronal cells resulted in an isoform-dependent transcriptional suppression of PKCδ expression without changes in the stability of mRNA and protein or DNA methylation. The reduction in PKCδ transcription was mediated, in part, through the suppression of constitutive NFκB activity targeted at two proximal PKCδ promoter κB sites. This occurred independently of NFκB/IκBα nuclear translocation, but was associated with decreased NFκB-p65 acetylation. Also, αsyn reduced p300 levels and its histone acetyl-transferase (HAT) activity, thereby contributing to diminished PKCδ transactivation. Importantly, reduced PKCδ and p300 expression also were observed within nigral dopaminergic neurons in αsyn transgenic mice. These findings expand the role of αsyn in neuroprotection by modulating the expression of the key proapoptotic kinase PKCδ in dopaminergic neurons.

Keywords

α-synuclein; PKCδ; apoptosis; Parkinson's disease; p300; NFκB

Introduction

Environmental neurotoxic insults and genetic defects in certain genes have been implicated in the etiology of PD (Dauer and Przedborski, 2003; Hatcher et al., 2008). Oxidative stress serves as a central mediator of degenerative processes in PD (Greenamyre and Hastings, 2004; Burke, 2008; Zhou et al., 2008); however, the key cell signaling mechanisms underlying oxidative damage to nigral dopaminergic neurons are not entirely clear. Our

Correspondence should be addressed to: Dr. Anumantha G. Kanthasamy, Parkinson's Disorder Research Laboratory, Department of Biomedical Sciences, Iowa State University, 2062 College of Veterinary Medicine Building, Ames, IA 50011. Telephone: (515) 294-2516. Fax: (515) 294-2315. akanthas@iastate.edu.

laboratory has been studying PKCδ-mediated cell death signaling in the oxidative damage of dopaminergic neurons. PKCδ, a novel PKC isoform, has been recognized as a key proapoptotic effector in various cell types (Brodie and Blumberg, 2003; Kanthasamy et al., 2003). The role of PKCδ in nervous system function is beginning to emerge, and we demonstrated that PKCδ is an oxidative stress-sensitive kinase that is persistently activated by caspase-3-dependent proteolytic cleavage to mediate dopaminergic neurodegeneration in cellular models of PD (Anantharam et al., 2002; Kanthasamy et al., 2003; Kaul et al., 2003). We showed that cytochrome C release and caspase-9 and caspase-3 activation serve as upstream events of the PKCδ-mediated cell pathway during mitochondrial impairment (e.g., MPP^+) in dopaminergic neuronal cells (Kaul et al., 2003). Importantly, depletion of PKCδ by siRNA or blockage of PKCδ activation by overexpression of a PKCδ kinase-dominant-negative mutant or caspase-cleavage-resistant mutant protects against multiple insults in cultured neurons (Kitazawa et al., 2003; Yang et al., 2004; Latchoumycandane et al., 2005). Furthermore, pharmacological inhibition of PKCδ prevents MPTP-induced degeneration of nigrostriatal dopaminergic neurons in animal models (Zhang et al., 2007a). We also showed that PKCδ inhibits tyrosine hydroxylase (TH) activity and dopamine synthesis in dopaminergic neurons (Zhang et al., 2007b). Despite the known proapoptotic function of PKCδ in dopaminergic neurons, the role of this kinase in cellular stress induced by proteins associated with familial-PD-linked genes is not known.

αSyn is a presynaptic protein predominantly expressed in neurons throughout the mammalian brain. The physiological functions of αsyn are poorly understood, but evidence has suggested a role for it in synaptic plasticity, dopamine synthesis, and membrane trafficking (Clayton and George, 1998; Perez et al., 2002; Outeiro and Lindquist, 2003). The relevance of αsyn to PD pathogenesis is based on case studies of familial PD resulting from mutations or multiplications of αsyn gene, as well as the observation that misfolded αsyn is a major constituent of Lewy bodies in both familial and sporadic PD (Spillantini et al., 1998; Norris et al., 2004). Although altered αsyn processing is thus considered a main determinant of PD, a growing body of evidence suggests a protective role of native αsyn in neurodegeneration (Manning-Bog et al., 2003; Sidhu et al., 2004; Chandra et al., 2005; Leng and Chuang, 2006; Monti et al., 2007).

While studying the PKCδ-dependent cell death mechanisms, we unexpectedly found striking neuroprotection in an αsyn-expressing dopaminergic cell model during exposure to the Parkinsonian neurotoxicant MPP^+. This led us to further investigate the molecular mechanisms underlying the neuroprotective function mediated by αsyn in dopaminergic neurons using cell culture and animal models. In the present study, we demonstrate a novel functional association between PKCδ and αsyn in which αsyn represses PKCδ expression by a mechanism involving modulation of both NFκB and p300 signaling pathways in a dopaminergic neuronal cell model and in transgenic αsyn mice. We also show that the deregulation of proapoptotic PKCδ expression protects dopaminergic neurons against MPP^+ toxicity. These observations extend the physiological role of native αsyn in protecting against neuronal injury.

Materials and Methods

Reagents

1-methyl-4-phenylpyridinium (MPP^+), actinomycin D (ActD), protein A/G beads, sodium butyrate, and mouse β-actin antibody were purchased from Sigma-Aldrich (St. Louis, MO). SN-50 peptide, garcinol, and N-(4-Chloro-3-trifluoromethyl-phenyl)-2-ethoxy-6-pentadecyl-benzamide (CTPB) were obtained from Enzo Life Sciences (Plymouth Meeting, PA). Biotin-16-UTP and the Cell Death Detection ELISA Plus assay kit were purchased from Roche Molecular Biochemicals (Indianapolis, IN). Z-DEVD-FMK was obtained from

Alexis Biochemicals (San Diego, CA). Acetyl-DEVD-amino-4-methylcoumarin (Ac-DEVD-AMC) was obtained from Bachem (King of Prussia, PA). The Bradford protein assay kit was purchased from Bio-Rad Laboratories (Hercules, CA). The DNeasy blood & tissue kit was obtained from Qiagen (Valencia, CA). Hoechst 33342, Lipofectamine Plus reagent, Lipofectamine 2000 reagent, hygromycin B, penicillin, streptomycin, fetal bovine serum, L-glutamine, RPMI 1640 medium, methionine-free RPMI 1640 medium, Neurobasal medium, B27 supplement, and Dulbecco's modified Eagle's medium were purchased from Invitrogen (Carlsbad, CA). Dynabeads M-280 was purchased from Dynal Biotech (Oslo, Norway). [^{3}H]Acetyl-CoA, poly (dI-dC), [^{35}S]-methionine, HRP-linked anti-mouse and anti-rabbit secondary antibodies, and the ECL chemiluminescence kit were obtained from GE Healthcare (Piscataway, NJ). Antibodies to PKCδ, PKCα, PKCβI, PKCζ, p65, p50, IκBα, CBP, p300, and αsyn (#sc-12767, only detecting αsyn of human origin) were purchased from Santa Cruz Biotechnology (Santa Cruz, CA); the rabbit polyclonal antibody for acetyl-lysine, mouse p300, and histone H3 antibodies were obtained from Milipore (Billerica, MA). αSyn monoclonal antibody detecting both human and rat origins was purchased from BD Biosciences (Syn-1, San Diego, CA); the mouse TH antibody was obtained from Chemicon (Temecula, CA); the goat polyclonal antibody for lactate dehydrogenase (LDH) and mouse monoclonal antibody for Lamin B1 were purchased from Abcam (Cambridge, MA). IRDye800 conjugated anti-rabbit secondary antibody was obtained from Rockland Labs (Gilbertsville, PA). Alexa 680-conjugated anti-mouse, Alexa 488-conjugated anti-mouse, Alexa 568-conjugated anti-rabbit secondary antibodies and mouse V5 antibody were obtained from Invitrogen. Anti-goat secondary antibody and normal rabbit IgG were obtained from Santa Cruz Biotechnology.

Plasmids

The plasmid encoding wild-type human αsyn protein (pCEP4-αsyn) was a kind gift from Dr. Eliezer Masliah (University of California, San Diego, CA). A control pCEP4 empty vector was purchased from Invitrogen. To prepare pLenti-V5-PKCδ and pLenti-V5-αsyn lentiviral vectors, full-length mouse PKCδ (gi: 6755081) and human αsyn (gi: 6806897) cDNA were PCR-generated from pGFP-PKCδ (kind gift of Dr. Mary E. Reyland) and pCEP4-αsyn with the following primer pairs, respectively. For PKCδ, forward, 5'-CACCATGGCACCCTTCCTGCGC-3', reverse, 5'-AATGTCCAGGAATTGCTCAAAC-3'; for αsyn, forward, 5'-CACCATGGATGTATTCATGAAAGGAC-3', reverse, 5'-GGCTTCAGGTTCGTAGTCTTG-3'. The PCR products were then subcloned in-frame into the C-terminal V5-tagged expression vector pLenti6/V5-TOPO (Invitrogen) as described (Kitazawa et al., 2005; Latchoumycandane et al., 2005). A control lentiviral construct pLenti-V5-LacZ, encoding β-galactosidase fused to the V5 epitope, was also obtained from Invitrogen. To generate pGL3-PKCδ promoter construct, rat genomic DNA was isolated using the DNeasy blood & tissue kit and used as template to amplify the 1.7 kb DNA fragment (−1700 to +22, +1 denotes the transcription start site) of rat PKCδ gene. PCR conditions used were 94°C for 45 sec; 30 cycles of 94°C for 30 sec, 64.6°C for 30 sec, and 72°C for 2 min; and 72°C for 10 min. Following PCR, the amplified product was cloned into the XhoI/HindIII sites of pGL3-Basic vector (Promega, Madison, WI). All constructs were verified by DNA sequencing.

Primary mesencephalic cultures and treatment

All of the procedures involving animal handling were approved by the Institutional Animal Care Use Committee (IACUC) at the Iowa State University. Primary mesencephalic neuronal cultures were prepared as described in our recent publications (Ghosh et al., 2010; Zhang et al., 2007c). Briefly, 24-well plates containing coverslips were coated overnight with 0.1 mg/ml poly-D-lysine. Mesencephalon tissue was dissected from gestational 14-day-

old mouse embryos and kept in ice-cold Ca^{2+}-free Hanks's balanced salt solution. Cells were then dissociated in Hank's balanced salt solution containing trypsin-0.25% EDTA for 30 min at 37 °C. After the incubation, 10% heat-inactivated fetal bovine serum in Dulbecco's modified Eagle's medium was added to inhibit trypsin digestion. The cells were triturated and suspended in Neurobasal medium supplemented with 2% Neurobasal supplement (B27), 500 μM L-glutamine, 100 IU/ml penicillin, and 100 μg/ml streptomycin, plated at 1×10^6 cells in 0.5 ml/well and incubated in a humidified CO_2 incubator (5% CO_2 and 37 °C). Half of the culture medium was replaced every 2 days, and experiments were conducted using between 6 and 7 day cultures. After exposure to the NFκB inhibitor SN50 and the p300 inhibitor garcinol or the activator CTPB for 24 h, the primary cultures were processed for immunocytochemical analysis.

Cell culture and stable expression of α-synuclein

Rat immortalized mesencephalic dopaminergic neuronal cell line ($1RB_3AN_{27}$, referred to as N27 cells) was a kind gift of Dr. Kedar N. Prasad (University of Colorado Health Sciences Center, Denver, CO). Rat striatal GABAergic M213-20 cell line was a generous gift from Dr. William Freed (National Institute on Drug Abuse, National Institutes of Health, Baltimore, MD). Mouse dopaminergic MN9D cell line was a kind gift from Dr. Syed Ali (National Center for Toxicological Research/FDA, Jefferson, AR). Rat pheochromocytoma PC12 dopaminergic cell line and human dopaminergic neuroblastoma SH-SY5Y cell line were obtained from the American Type Culture Collection (ATCC, Rockville, MD). N27 and PC12 cells were cultured as described (Zhang et al., 2007c). M213-20, MN9D, and SH-SY5Y cells were grown in Dulbecco's modified Eagle's medium supplemented with 10% fetal bovine serum, 2 mM L-glutamine, 50 units penicillin, and 50 units streptomycin.

To generate a stable cell line expressing the human wild-type αsyn, N27 cells were stably transfected with pCEP4-αsyn or pCEP4 empty vector by Lipofectamine Plus reagent according to the procedure recommended by the manufacturer and described (Kaul et al., 2005a). The stable transfectants were selected in 400 μg/ml of hygromycin and further maintained in 200 μg/ml of hygromycin added to N27 growth media.

Animals

Transgenic mice (stock number 008389) that express human wild-type αsyn under the control of the Thy-1 promoter (Andra et al., 1996) and non-carrier littermate control mice were purchased from the Jackson Laboratory (Bar Harbor, Maine). This line of transgenic animals has been characterized previously (Chandra et al., 2005). It expresses high levels of αsyn throughout the brain, but unlike some mutant transgenic lines, it does not display the Parkinson's like phenotype. Six- to eight-week-old male transgenic and non-carrier control mice were housed in standard conditions: constant temperature (22±1°C), humidity (relative, 30%), and a 12 h light/dark cycle with free access to food and water. Animal care procedures strictly followed the NIH Guide for the Care and Use of Laboratory Animals and were approved by the Iowa State University IACUC.

Immunoblotting and immunoprecipitation

Cell lysates were prepared as described previously (Zhang et al., 2007c). Nuclear and cytoplasmic extracts were isolated using the NE-PER nuclear and cytoplasmic extraction kit (Thermo Scientific, Waltham, MA). The protein concentrations were determined with the Bradford protein assay kit at 595 nm. Immunoblotting and densitometric analysis of immunoblots were performed as described previously (Kanthasamy et al., 2006). Briefly, the indicated protein lysates containing equal amounts of protein were fractionated through a 7.5%–15% SDS-polyacrylamide gel and transferred onto a nitrocellulose membrane (Bio-Rad Laboratories). Membranes were blotted with the appropriate primary antibody and

developed with HRP-conjugated secondary antibody followed by ECL detection. IRDye800 anti-rabbit or Alexa 680-conjugated anti-mouse antibodies were also used as secondary antibodies. The immunoblot imaging was performed with either a Kodak image station IS2000MM (Kodak Molecular Imaging System, Rochester, NY) or an Odyssey infrared imaging system (Li-cor, Lincoln, NE), and data were analyzed using one-dimensional image analysis software (Kodak Molecular Imaging System) or Odyssey software 2.0 (Li-cor). Blots were stripped and re-probed with anti-β-actin antibody as an internal control for loading.

For immunoprecipitation studies, briefly, cells were lysed in immunoprecipitation buffer (50 mM Tris-HCl, pH 7.4, 150 mM NaCl, 1 mM EDTA, 10 mM NaF, 1% Trition X-100, 1 × halt protease inhibitor cocktails), and the resultant lysates were incubated on ice for 15 min followed by centrifugation at 16,000 × *g* for 15 min. The supernatant fractions were then pre-cleared with protein A or protein G beads for 30 min at 4°C followed by centrifugation at 16,000 × *g* at 4 °C for 10 min. Five microgram of the indicated antibody along with 50 μl of 50% of protein A or protein G beads was added to the cell lysates and incubated overnight at 4 °C on a rotator. The immunoprecipitates were collected, washed extensively with cold PBS, and prepared for SDS/PAGE gel by addition of 2 × SDS sample buffer and then boiling for 10 min.

Transfections and infections

Transient transfections of αsyn-expressing and vector control N27 cells with promoter reporter were performed using Lipofectamine 2000 reagent in accordance with the manufacture's protocol. Cells were plated in 6-well plates at 4×10^5 cells/well one day before transfection. Four microgram of pGL3-PKCδ construct or pGL3-Basic empty vector was transiently transfected, and 0.5 μg of β-galactosidase vector (pcDNA3.1-βgal, Invitrogen) was added to each well to monitor transfection efficiencies. Twenty-four h post-transfection, the cells were lysed in 200 μl of report lysis buffer (Promega). Luciferase activity was measured on a luminometer (Reporter Microplate, Turner Designs, Sunnyvale, CA) using the Luciferase assay kit (Promega), and β-galactosidase activity was detected using the β-galactosidase assay kit (Promega). The ratio of luciferase activity to β-galactosidase activity was used as a measure of normalized luciferase activity.

Electroporation of small interfering RNAs (siRNAs) was conducted by using a Nucleofector device and the Cell line nucleofector kit (all from Lonza, Walkersville, MD) following the manufacturer's instructions. Specific αsyn siRNA (#16708) and scrambled negative control siRNA (#4611) were purchased from Ambion (Austin, TX). The p300-specific siRNA (#SI02989693) was purchased from Qiagen. The NFκB-p65-specific siRNA as described (Chen et al., 2006) was synthesized by Integrated DNA Technologies (Coralville, IA). The siRNA sequence for αsyn is 5'-GCAGGAAAGACAAAAGAGGtt-3' and for NFκB-p65 is 5'-GCAGUUCGAUGCUGAUGAAUU-3'. In each electroporation, 2×10^6 cells were resuspended in 100 μl of the electroporation buffer supplied with the kit, along with 1.3 μg of gene-specific siRNA or scrambled negative siRNA. The sample was then electroporated using the pre-set nucleofector program #A23 recommended by the manufacture. After electroporation, the cells were immediately transferred to pre-warmed culture medium. The next day media were replaced to normal growth media. Mock transfection with electroporation buffer alone was also included as a transfection control. After 72 h or 96 h from the initial transfection, the cell lysates were collected and analyzed using Western blotting to confirm the extent of αsyn, NFκB-p65, p300, and PKCδ expression. Where indicated, the cell nuclear extracts were prepared and used for EMSA analysis.

Lentiviral constructs (pLenti-V5-PKCδ, pLenti-V5-αsyn, or control construct pLenti-V5-LacZ) were packaged into virus *via* transient transfection of the 293FT packaging cell line

(Invitrogen) using Lipofectamine 2000 reagent, as described (Cooper et al., 2006). The lentivirus in the medium was collected by centrifuging at 72 to 96 h post-transfection. All transductions were performed at a multiplicity of infection (MOI) of 1 in the presence of polybrene (6 μg/ml). To assess the effect of transient human αsyn overexpression on PKCδ expression, N27 cells were infected with lentiviral particles encoding V5-αsyn or V5-LacZ for 48 h and collected for immunoblot analysis. To test the effects of restoring PKCδ expression on MPP^+ neurotoxicity, stable αsyn-expressing and vector control N27 cells were infected with PKCδ or control LacZ lentivirus for 24 h. The cells were then treated with fresh media containing 300 μM MPP^+ for 48 h prior to analysis. In experiments aimed at detecting the expression of pLenti-V5-PKCδ and pLenti-V5-LacZ, the cells were incubated with lentivirus for 48 h and collected for immunoblot analysis.

Caspases-3 activity and DNA fragmentation assays

Caspases-3 activity was measured as previously described (Kaul et al., 2005a). Briefly, after treatment with 300 μM MPP^+, cells lysates were prepared and incubated with a specific fluorescent substrate, Ac-DEVD-AMC (50 μM) at 37 °C for 1 h. Caspases-3 activity was then measured using a SpectraMax Gemini XS Microplate Reader (Molecular Devices, Sunnyvale, CA) with excitation at 380 nm and emission at 460 nm. The caspase-3 activity was calculated as fluorescence units per milligram of protein.

DNA fragmentation assay was performed using a Cell Death Detection ELSA plus kit as previously described (Anantharam et al., 2002). Briefly, after treatment with 300 μM MPP^+, cells were collected and lysed in 450 μl of lysis buffer supplied with the kit for 30 min at room temperature, and spun down at 2300 × *g* for 10 min to collect the supernatant. The supernatant was then used to measure DNA fragmentation as per the manufacture's protocol. Measurements were made at 405 and 490 nm using a SpectraMax 190 spectrophotometer (Molecular Devices).

Immunostaining and microscopy

After perfusion with 4% paraformaldehyde, the mice brains were removed, immersion fixed in 4% paraformaldehyde, and cryoprotected in sucrose. Then the brain was cut on a microtome into 20 μm sections. Sections from substantia nigra were used for dual-labeled immunofluorescence. After washing with PBS, the brain sections were rinsed with blocking buffer containing 2% BSA, 0.05% Tween-20, and 0.5% Triton X-100 in PBS for 45 min and then incubated overnight at 4°C with the following combinations of primary antibodies: anti-PKCδ (1:250, Santa Cruz) and anti-TH (1:1800, Chemicon), or anti-p300 (1:350, Santa Cruz) and anti-TH (1:1800, Chemicon), followed by incubation with anti-rabbit Alexa 568-conjugated (red, 1:1000) and anti-mouse Alexa 488-conjuated secondary antibodies (green, 1:1000) for 1 h at room temperature. After this, Hoechst 33342 (10 μg/ml) was added for 3 min at room temperature to stain the nucleus. The brain sections were mounted and observed with either an oil-immersion 63× PL APO lens with a 1.40 numerical aperture or an oil-immersion 100× PL APO lens with a 1.40 numerical aperture using a Leica SP5 X confocal microscope system (all from Leica, Allendale, NJ) at Confocal Microscopy and Image Analysis Facility at Iowa State University. For final output, images were processed using LAS-AFlite software (Leica). For computer-assisted image analysis, a 0.051 mm^2 area was delineated using this LAS-AFlite software and TH-PKCδ colocalized dopaminergic neurons were counted independently and blindly by two investigators. Data were expressed as either percent of TH-positive cells containing PKCδ immunoreactivity/total TH neurons or number of TH-positive cells containing PKCδ immunoreactivity/area (mm^2).

Immunostaining of PKCδ, TH, and αsyn was performed in primary mesencephalic neurons, αsyn-expressing and vector control N27 cells. Cells grown on coverslips pre-coated with

poly-L-lysine or poly-D-lysine were washed with PBS and fixed in 4% paraformaldehyde for 30 min. After washing, the cells were permeabilized with 0.2% Triton X-100 in PBS, washed with PBS, and blocked with blocking agent (5% bovine serum albumin, 5% goat serum in PBS). Cells were then incubated with the antibody against human αsyn (1:500, Santa Cruz), TH (1:1800, Chemicon), and PKCδ (1:1000, Santa Cruz) overnight. Fluorescently conjugated secondary antibody (Alexa-488-conjugated anti-mouse antibody, green, 1:1500, or Alexa 568-conjugated anti-rabbit antibody red, 1:1500) was used to visualize the protein. Nuclei were counterstained with Hoechst 33342 for 3 min at a final concentration of 10 μg/ml. Finally, images were viewed using an oil-immersion 60 × Plan Apo lens with a 1.45 numerical aperture on a Nikon inverted fluorescence microscope (model TE2000, Nikon, Tokyo, Japan). Images were captured with a SPOT color digital camera (Diagnostic Instruments, Sterling Heights, MI) and processed using Metamorph 5.07 image analysis software (Molecular Devices). For quantitative analysis of immunofluorescence, we measured average pixel intensities from the region of interest (ROI) using the Metamorph 5.07 image analysis software.

Pulse-chase assays

Before pulse-labeling, cells were starved of methionine for 30 min. Cells were subsequently pulse-labeled with methionine-free RPMI 1640 medium containing 125 μCi/ml [^{35}S]-methionine for 2 h. Afterwards, cells were rinsed twice with warm PBS, and chased in complete growth medium for various times up to 48 h. At different chase times, the cells were collected and subsequently subjected to immunoprecipitation using PKCδ antibody as described above. The immunoprecipitates were separated with 10% SDS-PAGE and analyzed by autoradiography at 24–48 h using a PhosphoImager (Personal Molecular Imager FX, Bio-Rad Laboratories). Band quantifications were processed using Quantity One 4.2.0 software (Bio-Rad Laboratories).

RT-PCR and methylation-specific PCR (MSP)

Total RNA was isolated and converted to cDNA using Absolutely RNA miniprep kit from Stratagene (La Jolla, CA) and High capacity cDNA archive kit from Applied Biosystems (Foster City, CA), respectively. For semiquantitative RT-PCR, 1 μl of the reverse transcriptase reaction mixture served as a template in PCR amplification. PCR amplifications were performed using the following program: 94 °C for 3 min; 35 cycles of 94 °C for 45 sec, 56 °C (PKCδ, η, and λ) or 60 °C (PKCα, ε, ζ, and GAPDH) for 30 sec, 72 °C for 45 sec. PCR products were then separated by electrophoresis in 1–2% agarose gel and visualized by ethidium bromide staining.

Quantitative real-time RT-PCR was performed using Brilliant SYBR Green QPCR Master Mix kit and the Mx3000P QPCR system (all from Stratagene). The p300 primer set was using a QuantiTect Primers assay (Qiagen, #QT01083859). The β-actin was used as an internal control for RNA quantity (sequence is listed in supplemental Table 1). The reaction mixture included 1 μl of cDNA (100 ng RNA used), 12.5 μl of 2 × master mix, 0.375 μl of reference dye, and 0.2 μM of each primer. Cycling conditions contained an initial denaturation at 95 °C for 10 min, followed by 40 cycles of 95 °C for 30 sec, 60 °C for 30 sec, and 72 °C for 30 sec. Fluorescence was detected during the annealing/extension step of each cycle. Dissociation curves were run to verify the singularity of the PCR product. The data were analyzed using the comparative threshold cycle method. Briefly, the relative PKCδ expression (expressed as fold differences) between αsyn-expressing and vector control N27 cells was calculated as $2^{-(\Delta CtSYN - \Delta CtVEC)}$, where ΔCt represented the mean Ct value of PKCδ or p300 after normalization to β-actin internal control.

For MSP experiments, genomic DNA was isolated from αsyn-expressing and vector control N27 cells using the DNeasy blood & tissue kit as mentioned earlier. Bisulfite modification was subsequently carried out on 500 ng of genomic DNA by the MethylDetector bisulfite modification kit (Active Motif, Carlsbad, CA) according to the manufacturer's instructions. Two pairs of primers were designed to amplify specifically methylated or unmethylated PKCδ sequence using MethPrimer software (Li and Dahiya, 2002). The cycling condition was: 94 °C for 3 min, after which 35 cycles of 94 °C for 30 sec, 52.5 °C for 30 sec, 68 °C for 30 sec, and finally 72 °C for 5 min. PCR products were loaded onto 2% agarose gels for analysis. Negative control PCRs were performed using water only as template.

Assessments of mRNA stability

The PKCδ mRNA decay experiments were conducted as described (Jing et al., 2005) with some modification. Briefly, cells were treated with 5 μg/ml actinomycin D to block *de novo* transcription, total RNA were isolated at selected time points thereafter, and the amount of PKCδ mRNA was determined by quantitative real-time RT-PCR. The PKCδ mRNA values were normalized to the amount of β-actin internal control in each sample and expressed as the percentage of mRNA levels present at time 0 (set to 100%) prior to the addition of actinomycin D.

Nuclear run-on assays

The nuclear run-on assays were performed with minor modifications to the method described by (Patrone et al., 2000). Nuclei were prepared from 60×10^6 cells by resuspending in 4 ml of Nonidet P-40 lysis buffer (10 mM Tris-HCl, pH 7.4, 3 mM $MgCl_2$, 10 mM NaCl, 150 mM sucrose and 0.5 % Nonidet P-40), and a 5-min incubation in ice followed. Nuclei were isolated by centrifugation, washed with cell lysis buffer devoid of Nonidet P-40, and the pellets were resuspended in 100 μl of freezing buffer (50 mM Tris-HCl, pH 8.3, 40 % glycerol, 5 mM $MgCl_2$ and 0.1 mM EDTA). One volume of transcription buffer (200 mM KCl, 20 mM Tris-HCl, pH 8.0, 5 mM $MgCl_2$, 4 mM dithiothreitol, 4 mM each of ATP, GTP and CTP, 200 mM sucrose and 20% glycerol) was added to nuclei. Eight μl of biotin-16-UTP was then supplied to the mixture. After incubation for 30 min at 29 °C, the reaction was terminated and total RNA was purified using the Absolutely RNA miniprep kit according to the manufacturer's instructions. RNA was eluted in 60 μl of nuclease-free water and 10 μl was saved as total nuclear RNA. Dynabeads M-280 (50 μl) was subsequently used to capture the run-on RNA. Three μl of run-on RNA or 10 μg total nuclear RNA was subjected to cDNA synthesis and quantitative real-time PCR as described above. To monitor undesired RNA capture by Dynbeads, control reactions were also performed in which conditions were identical except that UTP was added to the transcription system in the place of biotin-16-UTP.

Electrophoretic mobility shift assays (EMSA)

Nuclear and cytoplasmic proteins were prepared using the NE-PER nuclear and cytoplasmic extraction kit as described before. The IRye™700-labeled oligos PkcδNFκBs and NFκB, corresponding to the NFκB-like sequences within the rat PKCδ promoter and the consensus sequence of NFκB respectively, were synthesized by Li-cor and used as labeled probes. The unlabeled competitor oligos were obtained from Integrated DNA Technologies. All oligos sequences are illustrated in supplemental Table 2. Protein-DNA binding reactions were performed with 5–10 μg of nuclear or cytoplasmic proteins, 1 μl of labeled oligonucleotide (50 fmol) in a total volume of 20 μl of mixture containing 10 mM Tris-HCl (pH 7.5), 50 mM NaCl, 0.25% Tween−20, 2.5 mM dithiothreitol (DTT), 0.05 mM EDTA, and 1 μg of poly (dI-dC). After incubation at room temperature for 20 min, the resulting DNA-protein complexes were resolved on a 6.6% non-denaturing polyacrylamide gel at 10 V/cm for about 50 min at 4 °C in 1 × TGE buffer. Gels were analyzed on the Odyssey infrared

imaging system (Li-cor). In competition experiments, before the addition of the labeled probe, nuclear extracts were pre-incubated for 30 min at room temperature with a 100-fold molar excess of unlabeled competitor oligos. In super shift experiments, 400 ng of anti-p50, anti-p65, or normal rabbit IgG was incubated with nuclear extracts for 30 min at room temperature prior to the addition of labeled probe.

Histone acetyltransferase activity assays

p300 HAT activity was measured using a p300/CBP immunoprecipitation HAT assay kit from Millipore following the manufacture's protocol with minor modifications as previously described (Nakatani et al., 2003). Briefly, one milligram of nuclear extracts from αsyn-expressing and vector control N27 cells were precipitated with 5 μg of anti-p300 antibody or normal mouse IgG and 50 μl of magnetic protein-G beads (Active Motif) at 4°C overnight. The collected beads were washed with three times cold PBS and incubated with HAT assay cocktail (50 μl) containing 10 μl of core histones and 100 μM [^{3}H]acetyl-CoA (0.5 μCi/μl) at 30 °C for 30 min. Fifteen μl of the supernatant of each sample was placed on P81 square papers and [^{3}H]acetyl incorporation into the substrates was measured using a scintillation counter. Data were expressed as mean values of counts, subtracted from background values measured in samples containing normal mouse IgG.

Chromatin immunoprecipitation assays (ChIP)

The ChIP-IT Express enzymatic kit from Active Motif was used to analyze the *in vivo* binding of NFκB p65 and p50 subunits, and p300/CBP co-activators onto the rat PKCδ promoter region. Unless otherwise stated, all reagents, buffers, and supplies were included in the kit. The ChIP assays were performed following the manufacture's instructions with slight modifications. Briefly, ~1.5×10^7 cells were fixed in 1% formaldehyde for 10 min at room temperature. After cross-linking, the nuclei were prepared and chromatin was enzymatic digested to 200–1500 bp fragments (verified through running on a 1% agarose gel) by incubation with the enzymatic shearing cocktail for 12 min at 37 °C. The sheared chromatin was collected by centrifuge, and a 10-μl aliquot was saved as an input sample. Aliquots of 70-μl sheared chromatin were incubated overnight with rotation at 4 °C with protein G magnetic beads and three μg indicated antibody. Equal aliquots of each chromatin sample were saved for no-antibody controls. After extensive washing, reversal of cross-links, and proteinase K digestion, the elute DNA in the immunoprecipitated samples was directly collected on a magnetic stand, and the input DNA was purified by phenol/chloroform extraction and ethanol precipitation. The DNA samples were analyzed by PCR using primer pairs designed to amplify a region (−103 to +60) within PKCδ promoter. Conditions of linear amplification were determined empirically for the primers. PCR conditions are as follows: 94 °C 3 min; 94 °C 20 sec, 58 °C 30 sec, and 72 °C 30 sec for 35 cycles. The PCR products were resolved by electrophoresis in a 1.0% agarose gel and visualized after ethidium bromide staining.

Bioinformatics

CpG island identification was analyzed with the web-based program CpG Island Searcher (Takai and Jones, 2002). This program defines a CpG island as a region with a G+C content ≥ 50%, longer than 200 bp nucleotides, and an Observation/Expectation CpG ratio > 0.6. The search for the phylogenetic sequence conservation among rat, human, murine, and cow PKCδ promoter was conducted with the DiAlign professional TF Release 3.1.1 (DiAlign TF) (Morgenstern et al., 1996; Morgenstern et al., 1998) (Genomatix Software, Munich, Germany). This program identifies common transcription factor binding sites matches located in aligned regions though a combination of alignment of input sequences using multiple alignment program DiAlign (Morgenstern et al., 1996; Morgenstern et al., 1998) with recognition of potential transcriptional factor binding sites by MatInspector software

(Cartharius et al., 2005) (Genomatix Software), which employed matrices library version 8.0.

Data analysis

All statistical analyses were performed using the Prism 4.0 software (GraphPad Software, San Diego, CA). In PKCδ protein and mRNA degradation experiments, a one-phase exponential decay model was fitted to each data set using the nonlinear regression analysis program of Prism 4.0 software as follows: $Y = \text{Span } e^{-Kt} + \text{Plateau}$, where Y starts at Span + Plateau and decays with a rate constant K. The half-life of the each mRNA or protein was subsequently determined by 0.693/K. The goodness-of-fit was assessed as the square of the correlation coefficient (R^2). Data were analyzed either by Student's t test or one-way ANOVA followed by Tukey's pairwise multiple comparison test. Statistical significance was defined as $p<0.05$.

Results

Expression of human α-synuclein in N27 dopaminergic cells down-regulates PKCδ expression in an isoform-specific manner

We previously reported that PKCδ serves as a key proapoptotic effector in dopaminergic neurons, and caspase-3-mediated proteolytic cleavage of PKCδ is a key mediator in multiple models of dopaminergic neurodegeneration (Anantharam et al., 2002; Kaul et al., 2003; Yang et al., 2004; Kaul et al., 2005b; Kanthasamy et al., 2006; Zhang et al., 2007a). Growing evidence indicates that the neuroprotective mechanism of endogenous αsyn involves deregulation of gene expression of specific stress-signaling molecules linked to neuronal survival (Alves Da Costa et al., 2002; Hashimoto et al., 2002; Manning-Bog et al., 2003; Albani et al., 2004). Analysis in a variety of cell lines, MN9D, N27, PC12, M213-20, and SH-SY5Y, revealed a striking inverse correlation between PKCδ and αsyn protein levels (data not shown). These observations raised the question of whether αsyn might regulate PKCδ expression and thereby promote cell survival. To address this hypothesis, we engineered rat-immortalized mesencephalic dopaminergic N27 cell line to express human wild-type αsyn by stably transfecting with plasmid pCEP4-αsyn or pCEP4 control vector. The widely used N27 neuronal cell model represents a homogeneous population of TH-positive dopaminergic cells and is highly useful for studying degenerative mechanisms in PD (Clarkson et al., 1999; Kaul et al., 2005b; Peng et al., 2005a; Zafar et al., 2007; Zhang et al., 2007c; Lee et al., 2009). The stable expression of human αsyn in stable N27 cells was assessed by Western blot assay using the αsyn antibody (Syn-1) that detects both exogenously expressed human αsyn and endogenous rat αsyn. As shown in Fig. 1*A*, the αsyn endogenous level was too low to be detected in vector control N27 cells, whereas exogenously expressed αsyn could readily be detected in the αsyn-expressing N27 cells. Importantly, the level of αsyn achieved in αsyn-expressing N27 cells appears to be within the physiological range, as this level was comparable to that seen in the rat brain substantia nigra (rSN) homogenates (Fig. 1*A*). Further analysis of subcellular localization of αsyn in the stable cells demonstrated that αsyn is exclusively in the cytoplasm but absent in the nucleus (Supplemental Fig. 1). We next determined whether αsyn affects PKCδ expression. Western blot analysis (Fig. 1*B*, left panel) of various PKC isoforms showed a selective suppression of PKCδ in αsyn-expressing N27 cells. Quantitative analysis showed that αsyn caused a ~50% reduction in PKCδ protein levels, whereas PKCα, βI, and ζ were not affected (Fig. 1*B*, right panel). To further determine whether this specific inhibition occurred at the mRNA level, semiquantitative RT-PCR (primer sequences are listed in supplemental Table 1) was carried out (Fig. 1*C*, left panel). Similar to the trend seen in protein levels, only PKCδ mRNA expression was markedly reduced by αsyn. qRT-PCR analysis revealed a dramatic ~80% reduction in PKCδ mRNA in αsyn-expressing N27 cells (Fig. 1*C*, right

panel). To ensure the observed down-regulation of PKCδ gene expression in these two stable cell lines was not an artifact from the selection or maintenance of stable transfectants, we examined the PKCδ expression in transiently transduced N27 cells. As shown in Fig. 1*D*, transient transduction of N27 cells with lentivirus encoding human wild-type αsyn-V5 fusion also resulted in a dramatic decrease in expression of PKCδ gene compared with control lentivirus (lacZ-V5)-infected cells. Taken together, these data demonstrate that αsyn is capable of repressing the PKCδ isoform in N27 dopaminergic cells.

Dysregulation of PKCδ by α-synuclein protects against MPP^+-induced cell death in dopaminergic N27 cells

After we identified that increased αsyn inhibits the steady-state level of PKCδ, we investigated the significance of PKCδ downregulation by αsyn. Previously, we established the proapoptotic function of PKCδ in dopaminergic neurons using siRNA and dominant negative PKCδ mutants (Yang et al., 2004; Kitazawa et al., 2005; Latchoumycandane et al., 2005). In the present study, we employed a lentivirus encoding PKCδ fused to the V5 epitope (PKCδ-V5) to markedly overexpress PKCδ and investigated whether PKCδ gain of function influences the neurotoxicity in N27 cells following MPP^+ treatment. The increased expression of PKCδ after lentiviral infection compared with control lentivirus-infected cells (LacZ) was confirmed by Western blot assay (data not shown). The extent of MPP^+-induced apoptosis was measured by DNA fragmentation (Fig. 2*A*, left panel) and caspase-3 enzymatic activity (Fig. 2*A*, right panel) analysis. In LacZ control-infected cultures, αsyn-expressing N27 cells almost completely suppressed MPP^+-induced DNA fragmentation and caspase-3 activity as compared to vector control N27 cells. Importantly, introduction of PKCδ significantly increased MPP^+-induced DNA fragmentation ($p<0.01$) and caspase-3 activity ($p<0.05$) in αsyn-expressing N27 cells. These results suggest that downregulation of PKCδ by αsyn is protective. In further support of these data, MPP^+-induced PKCδ proteolytic cleavage and its nuclear translocation, events associated with apoptosis (Anantharam et al., 2002; DeVries et al., 2002; Kaul et al., 2003; Kaul et al., 2005b), were almost completely diminished in αsyn-expressing N27 cells compared to vector control N27 cells (Fig. 2*B*).

Next, we examined the localization of αsyn in the stable cells following MPP^+ treatment. As shown in Fig. 2*C*, the exclusive localization of αsyn in the cytoplasm was not affected by MPP^+, as determined by Western blot and immunostaining. Interestingly, a recent study demonstrates that subcellular localization of αsyn may contribute to its neurotoxicity: nuclear localization of αsyn promotes apoptosis whereas cytoplasmic localization of αsyn protects cells (Kontopoulos et al., 2006). Taken together, these results support a model in which αsyn acts in the cytoplasm to protect against MPP^+-induced dopaminergic cell death *via* negative regulation of the proapoptotic kinase PKCδ expression.

Increased α-synuclein expression in an animal model is associated with decreased PKCδ levels within nigral dopaminergic neurons

We further extend our findings from a dopaminergic cell culture model to an animal model. Since recent studies conducted in our laboratory demonstrated that PKCδ is expressed in dopaminergic neurons in nigral regions of the brain (Zhang et al., 2007c), we decided to determine whether an inverse relationship between αsyn and PKCδ expression in nigral dopaminergic neurons existed *in vivo*. For this purpose, we carried out immunohistological studies in transgenic mice that overexpress wild-type human αsyn (htg) and in non-transgenic control (non-tg) mice. This transgenic line has been characterized previously (Chandra et al., 2005); it expresses high levels of αsyn throughout the brain under the regulatory control of the Thy-1 promoter, and unlike some similar mutant transgenic lines, it does not display the Parkinson's like phenotype upon aging. This mouse line also displayed

a dramatic resistance to the neurodegeneration caused by deletion of cysteine-string protein-α (CSPα) (Chandra et al., 2005). The effects of overexpression of αsyn on PKCδ expression within nigral dopaminergic neurons were studied by double-immunostaining nigral tissues for TH (marker of dopaminergic neurons) and PKCδ. As shown in Fig. 3*A*, a strong PKCδ immunoreactivity (stained in red) was observed in control mice in the cytoplasm of TH-expressing neurons (stained in green). Moreover, the majority of the TH neurons displayed co-localization of TH and PKCδ (yellow color in the merged panel). In contrast, the αsyn transgenic mice exhibited a significant decrease in PKCδ immunoreactivity within TH neurons as well as significant loss of the corresponding co-localization of TH and PKCδ. Quantitative analysis of TH-PKCδ co-localized dopaminergic neurons relative to the number of total TH neurons showed that >70% of TH-positive cells lost their PKCδ expression in αsyn transgenic mice (Fig. 3*B*) as compared to control mice. Similar results were obtained by quantifying TH-PKCδ co-localized dopaminergic neurons in a delineated area (data not shown). Western blot analysis confirmed a ~6-fold increase in the levels of αsyn in the substantia nigra of αsyn transgenic mice (Fig. 3*C*). Overall, these results establish an *in vivo* relevance of the relationship between αsyn overexpression and PKCδ expression in dopaminergic neurons.

α-Synuclein attenuates PKCδ promoter activation and transcription efficiency without affecting PKCδ protein turnover or mRNA stability

We next investigated the molecular mechanism underlying the αsyn-induced suppression of PKCδ expression. First, we examined whether αsyn could destabilize PKCδ protein in N27 cells. To this end, we investigated the PKCδ turnover rate by performing a pulse-chase experiment on both αsyn-expressing and vector control N27 cells labeled with [^{35}S]-methionine. αSyn had no effect on PKCδ protein turnover (Fig. 4*A*). The relative half-life of PKCδ was estimated to be 14.77 h in vector control and 14.07 h in αsyn-expressing N27 cells (degradation rate constant K= 0.055±0.017 per hour in vector control cells vs. 0.051±0.007 per hour in αsyn-expressing cells), an insignificant difference between the two cells. We also considered the possibility that αsyn might directly alter the PKCδ mRNA instability. To address this possibility, we measured PKCδ mRNA half-life by treating cells with the transcription inhibitor ActD for 0–12 h, and quantified PKCδ mRNA by qRT-PCR (Fig. 4*B*). The relative half-life of PKCδ mRNA was about 2 h in vector control cells, and the decay continued thereafter. Notably, overexpression of αsyn did not change the relative half-life of PKCδ mRNA (degradation rate K=0.396±0.039 per hour in vector cells vs. 0.415±0.058 per hour in αsyn-expressing cells). Taken together, these results demonstrate that αsyn-induced suppression of PKCδ is not due to altered rate of PKCδ protein or mRNA decay, suggesting that there are no post-transcriptional effects of αsyn on PKCδ expression.

We therefore turned our attention to transcriptional steps that could mediate the reduction in PKCδ *via* αsyn. We first examined whether αsyn caused a decrease in the PKCδ promoter activity. For this, a 1.7 kb (−1700/+22, relative to the transcription start site) region of the rat PKCδ promoter was amplified and cloned into the pGL3-Basic reporter vector. The promoter activity was then studied by transfecting αsyn-expressing and vector control N27 cells with the reporter construct pGL3-PKCδ carrying PKCδ promoter. As shown in Fig. 4*C*, compared with vector control cells, αsyn resulted in a significant decrease ($p<0.001$) in luciferase activity, suggesting that αsyn-induced suppression of PKCδ is most likely mediated at the level of transcription.

Next, we employed a nuclear run-on assay to investigate the effects of αsyn on PKCδ transcriptional rate. In this assay, nuclei were isolated from either αsyn-expressing or vector control N27 cells and used with the reaction containing biotin-16-UTP. We also prepared nuclei from vector control cells and incubated without biotin-16-UTP as a negative control for the run-on reaction. After the transcriptional reaction, total nuclear RNA was extracted,

and then biotinylated RNA was isolated using Streptavidin magnetic beads. qRT-PCR analysis was conducted with the biotinylated RNA and total nuclear RNA pools. Fig. 4*D* shows the representative amplification plots for PKCδ mRNA (left panel) and β-actin mRNA (right panel). The amount of biotinylated PKCδ mRNA generated in nuclei from αsyn-expressing cells was lower than that obtained from vector control cells, but β-actin mRNA levels were nearly identical, indicating that αsyn specifically inhibits the PKCδ transcriptional rate. Quantitative analysis showed a significant reduction ($p<0.001$) in the PKCδ transcription efficiency in αsyn-expressing cells (Fig. 4*E*). Collectively, the results of the run-on experiment, combined with the promoter reporter analysis, strongly suggest the involvement of a transcriptional repression mechanism in the regulation of PKCδ expression. In addition, we also explored the possibility that epigenetic mechanisms such as DNA methylation (Supplemental Fig.2*A*) may be responsible for the α-syn-induced reduction in PKCδ. Examination of the methylation status of the rat PKCδ promoter by MSP analysis (Supplemental Fig. 2*B*) revealed an identical methylation pattern in α-syn-expressing and vector cells, suggesting that the hypermethylation mechanism is less likely to be involved in the repression of PKCδ.

Increased α-synuclein expression suppresses PKCδ in part by blocking NFκB activation

To further explore the mechanism of αsyn inhibition of the PKCδ promoter activity, the rat PKCδ proximal promoter (−178 to +22) was aligned for comparison with the homologous sequences from the murine, human, and bovine genome (Supplemental Fig. 3). Murine PKCδ and human PKCδ promoters were well conserved from 89% to 71% compared with rats, although the same region was less conserved in the bovine PKCδ gene (59%). Further analysis revealed six highly conserved transcription factor binding sites (TFBS) in the proximal promoter (Supplemental Fig. 3). Among these conserved TFBS, the most notable were two potential NFκB binding sites, located at positions −20 to −8 (designated as PkcδNFκB1) and −50 to −38 (designated as PkcδNFκB2). They are in close proximity, providing an enticing platform for NFκB binding and transactivation of the PKCδ gene. Additionally, a previous report indicated that NFκB may be involved in mouse PKCδ expression (Suh et al., 2003). Therefore, we carried out detailed studies on the role of these two κB sites in the regulation of basal PKCδ expression in N27 cells and also elucidated whether NFκB plays a role in αsyn-mediated downregulation of PKCδ expression. To determine if these sites were able to bind NFκB, we performed EMSA using PKCδ promoter's κB site sequence as a probe and nuclear extracts from vector cells as a source of NFκB (oligonucleotides sequences used in EMSA are listed in supplemental Table 2). As shown in Fig. 5*A*, in the absence of nuclear extract, the labeled probe is detected as free probe migrating at the gel front (lane 1). In contrast, in the presence of nuclear extract, an intense shifted band is seen in EMSA using PkcδNFκB1 (left panel) or PkcδNFκB2 (right panel) as a probe (Fig. 5*A*, lane 2). Sequence specificity of the DNA-protein complex was shown by competition with excess of selected unlabeled oligos. The addition of excess unlabeled self oligos, or NFκB consensus oligos, resulted in the ablation of this DNA-protein complex (Fig. 5*A*, lane 3 and 5). However, an excess of unlabeled mutant PkcδNFκB oligos, or unrelated AP1 consensus oligos, did not interrupt the binding of nuclear proteins (Fig. 5*A*, lane 4 and 6). In addition, parallel EMSA using NFκB consensus sequence as probe also confirmed that the PKCδ promoter-specific κB sites can compete efficiently against the NFκB consensus sequence for binding NFκB (data not shown). Thus, these data clearly demonstrate that the PKCδ promoter has two functional NFκB binding sites.

To further characterize NFκB binding to the PKCδ promoter, we performed supershift assay using PkcδNFκB1 as a probe and nuclear extracts from vector cells. As shown in Fig. 5*B*, in the absence of antibodies, NFκB binding to the PkcδNFκB1 probe was again observed (lane 1), and competition with an excess of self oligos was included as an internal control (lane 2).

In the presence of anti-p65 antibody, the protein-DNA complex was interrupted, and a specific supershift band was formed (lane 4). This effect was also observed with the complete ablation of protein-DNA complex and the formation of an intense supershift band when we added anti-p65 and anti-p50 together (lane 5). In the presence of anti-p50 antibody alone, however, no supershift was formed but the protein-DNA complex was significantly reduced (lane 3). The lack of a clear supershift with p50 antibody may be due to the interruption of the formation of protein-DNA complex by exposure to a specific antibody (Gustin et al., 2004). Normal rabbit IgG antibody displayed no effect on the formation of the protein-DNA complex. Thus, our data demonstrated that NFκB is constitutively activated in N27 cells, and that the activated NFκB bound to the PKCδ promoter comprised of a p50/p65 heterodimer.

If αsyn inhibits the PKCδ promoter activity through the NFκB *cis*-elements at the PKCδ promoter, we should see a decrease in the NFκB-DNA complex in αsyn-expressing cells. As expected, the nuclear extracts (both 5 μg and 10 μg) from αsyn-expressing cells exhibited reduced DNA binding activity to the PkcδNFκB1 probe as compared with vector control cells (Fig. 5*C*). A similar result was obtained when the labeled PkcδNFκB2 probe was used (data not shown). Based on these findings, we then carried out a ChIP assay to analyze the effect of αsyn on NFκB activation *in vivo*. As shown in Fig. 5*D*, αsyn expression diminished endogenous binding of both p65 and p50 to the PKCδ promoter. No detectable signal was observed in the absence of antibody in the immunoprecipitation process. To further confirm the inhibitory effect of αsyn on NFκB transactivation, parallel studies employing RNA interference to down-regulate αsyn were performed. For this study, we transfected siRNA-αsyn (si-αsyn) into αsyn-expressing cells and then examined the NFκB binding to the PKCδ promoter's κB element at 72 h post-transfection. EMSA showed that NFκB activity was dramatically increased in αsyn knockdown samples (Fig. 5*E*). The efficacy of αsyn-siRNA was evaluated by Western blot, and a 90% reduction in the α-syn level was obtained as compared to the negative control siRNA and mock transfected control (data not shown). Finally, we characterized the requirement of NFκB for constitutive PKCδ expression in N27 cells. To this end, we utilized NFκB-p65 siRNA to directly inhibit the p65 protein. When N27 cells were transfected with siRNA-p65 (si-p65), a ~56% reduction in the p65 level was observed, correlating with a concomitant ~35% decrease in the PKCδ protein level. However, the negative control siRNA and mock transfection control did not show a significant effect on the levels of p65 or PKCδ proteins (Fig. 5*F*). Collectively, these results indicate that NFκB plays an important role in PKCδ transactivation in N27 cells, and that αsyn-induced down-regulation of PKCδ expression was mediated, at least in part, by reducing the NFκB binding to κB enhancer elements at the PKCδ promoter.

To further confirm the functional role of NFκB in the regulation of PKCδ gene expression in primary dopaminergic neurons, mouse primary mesencephalic cultures were treated with the NFκB inhibitor SN-50, a cell permeable peptide that blocks NFκB nuclear translocation (de Erausquin et al., 2003), and PKCδ immunoreactivity of TH-positive neurons was analyzed immunocytochemically (Fig. 6). Exposure of primary mesencephalic cultures to SN-50 (100 μg/ml) for 24 h induced a significant reduction in PKCδ immunoreactivity in TH-positive neurons (Fig. 6*A*). Analysis of fluorescent intensity with Metamorph Image analysis software revealed a ~70% ($p<0.01$) decrease in PKCδ immunoreactivity in SN-50-treated TH-positive neurons (Fig. 6*B*). Also, the SN-50 (100 μg/ml) treated culture showed reduced p65 level in the nucleus, confirming the inhibitory effect of SN50 on NFκB activation (data not shown). These results confirm that NFκB is an important regulator of PKCδ expression in cultured substantia nigral neurons, and thus, further analyses were carried out to examine the mechanism of action of αsyn in inhibiting NFκB activity to down-regulate PKCδ expression.

α-Synuclein-induced blockade of NFκB activation is associated with decreased acetylation of p65, but does not correlate with alteration of nuclear translocation or protein levels of NFκB/IκBα

Our next objective was to explore the molecular basis of inhibition of NFκB activity by αsyn. Since αsyn is predominantly located in the cytoplasm (Supplemental Fig. 1), the inhibitory effect of αsyn on NFκB activity may be due to its interaction with NFκB in the cytoplasm, preventing NFκB localization to the nucleus. However, in our experimental conditions, we were unable to detect physical interactions between αsyn and NFκB subunits or IκBα by co-immunoprecipitation analysis (data not shown). It may also be possible for αsyn to indirectly modulate NFκB activity by enhancing the cytoplasmic retention of p50/p65 or altering cellular pools of IκBα. To test this possibility, the subcellular distribution of NFκB p50/p65 and IκBα was compared between αsyn-expressing cells and vector control N27 cells. Surprisingly, αsyn did not have any effect on p50/p65 NFκB subunits or IκBα in both cytoplasmic and nuclear fractions (Fig. 7*A*). To further determine if reduced NFκB/DNA binding activity by αsyn resulted from alteration of protein levels of NFκB subunits and IκBα, we analyzed p65, p50, and IκBα by Western blot. As shown in Fig. 7*B*, the total protein levels of p65, p50, and IκBα were not affected by αsyn either.

Studies were then undertaken to determine whether αsyn-mediated downregulation of NFκB activity might be related to NFκB/p65 acetylation, a nuclear event associated with increased transactivation potential of NFκB and regulated by both p300/CBP HAT and HDAC3 (Chen et al., 2001; Chen et al., 2002). In this experiment, whole cell extracts were immunoprecipitated with a p65 antibody, and acetylated p65 (Ac-p65) was detected by Western blot using an antibody specific for acetylated lysine. Total p65 proteins from immunoprecipitates were then re-probed with the p65 antibody. As shown in Fig. 7*C*, a ~65kDa acetylated p65 showed no overt differences in acetylated p65, but the total p65 levels immunoprecipitated from αsyn-expressing cells were significantly higher than that from vector control cells, which might be due to the different efficiencies achieved during immunoprecipitation steps. Quantification of normalized data (Ac-p65 over total p65) revealed a significant ($p<0.01$) reduction in Ac-p65 in αsyn-expressing cells compared to vector control cells (Fig. 7*C*, right panel). To further confirm the role of p65 acetylation in the modulation of PKCδ expression, we employed the HDAC inhibitor sodium butyrate, which increased the acetylation of p65 (Duan et al., 2007), possibly by inhibiting HDAC3. We previously reported that certain neurotoxic insults induce PKCδ cleavage *via* a caspase-3 dependent manner (Kaul et al., 2003; Kaul et al., 2005b). Since we have found that sodium butyrate markedly induced caspase-3-dependent cleavage of PKCδ in N27 cells (data not shown), a caspase-3-specific inhibitor Z-DEVD-FMK was applied to prevent the sodium butyrate-induced PKCδ cleavage. After co-treatment with sodium butyrate (1 mM) and Z-DEVD-FMK (50 μM) in αsyn-expressing cells, as expected, total cellular acetylation was significantly enhanced. In particular, two most prominent bands were observed at 15 kD and 10 kD, respectively (Fig. 7*D*, right panel). In correlation with this finding, sodium butyrate treatment resulted in a time-dependent increase in PKCδ protein levels, whereas it had no such effect on the levels of other PKC isoforms (α, βI, ζ), suggesting that increased cellular acetylation can isoform-specifically up-regulate PKCδ (Fig. 7*D*, left panel). Taken together, these results suggest that αsyn inhibition of NFκB binding to the PKCδ promoter is associated with decreased acetylation of p65, without alteration of NFκB nuclear translocation, IκBα degradation, or NFκB/IκBα protein levels.

α-Synuclein down-regulates p300 proteins, resulting in decreased p300 HAT activity and inhibition of p300-dependent transactivation of PKCδ expression

Because the acetylation of p65 by HATs p300/CBP plays a crucial role in NFκB activation, we hypothesized that p300/CBP may be a target for αsyn to inhibit p65 acetylation. First, to

determine what effect, if any, αsyn would exert on these proteins, we measured levels of p300 and CBP by Western blot. As illustrated in Fig. 8*A*, the amount of nuclear p300 was strikingly reduced (60%) in αsyn-expressing cells, whereas CBP was unaltered, suggesting a selective decrease in p300 proteins by αsyn. Neither p300 nor CBP can be detected in cytoplasmic fractions as they are predominantly nuclear proteins. To further examine whether the decrease in p300 proteins was at the mRNA level, the p300 mRNA was measured by qRT-PCR analysis. However, p300 transcript levels were unaffected by αsyn (data not shown), suggesting that other mechanisms, such as protein degradation, may be required for the decrease in p300 proteins. Next, we assessed the effect of reduced p300 on its HAT activity. In this experiment, p300 HAT activity was determined using an *in vitro* acetylation of the core histone with endogenous p300 proteins immunoprecipitated from αsyn-expressing and vector control cells. As shown in Fig. 8*B*, p300 HAT activity decreased by ~70% in αsyn-expressing cells as compared to vector cells, suggesting that the balance between HAT and HDAC activities in αsyn-expressing N27 cells was altered by αsyn. The reduction in p300 HAT activity by αsyn therefore appears to be at least in part a consequence of the depletion of p300 protein in αsyn-expressing cells. In addition to their intrinsic acetyltransferase activity, p300 and CBP are well-known for their roles in bridging multiple sequence-specific transcription factors to general transcriptional machinery to initiate transcription (Chan and La Thangue, 2001). Based on this understanding and our observation of decreased levels of p300 induced by αsyn, we were interested in determining whether αsyn could modulate p300 transactivation potential by disrupting p300 recruitment to the PKCδ promoter. To address this issue, we evaluated p300 binding to the PKCδ promoter by ChIP assay. Chromatin was immunoprecipitated with a p300 antibody and analyzed by PCR amplification of the PKCδ promoter region encompassing the κB binding sites. As shown in Fig. 8*C*, a small amount of p300 binding onto the PKCδ promoter was detected in vector control cells, whereas in αsyn-expressing cells, it was completely abolished (lane 4 *versus* 5). This effect was specific to p300, as binding and recruitment of CBP to the PKCδ promoter was not affected by αsyn (Fig. 8*C*, lane 2 *versus* 3). While these experiments demonstrated that αsyn blocked p300 association to the PKCδ promoter, they do not clarify a functional link between loss of p300 and αsyn repression of PKCδ. Therefore, we decided to utilize siRNA-p300 to directly inhibit endogenous p300 function. As shown in Fig. 8*D*, the transfection of siRNA-p300 (si-p300) into N27 cells resulted in a ~50% reduction in p300 protein, which was correlated with a concomitant ~50% decrease in the PKCδ protein level. Collectively, these results provide direct evidence for a specific loss of p300 protein and a subsequent decrease in HAT activity due to stable expression of αsyn, which could account for decreased p65 acetylation and binding activity, as well as down-regulation of recruitment and binding of p300 to the PKCδ promoter, which is at least partly responsible for the reduction in PKCδ expression.

We further examined the role of p300 HAT in controlling PKCδ expression in primary dopaminergic neurons using the pharmacological modulators of p300. Garcinol, a polyisoprenylated benzophenone derivative isolated from *Garcinia indica*, has been shown to potently inhibit the activity of p300 and PCAF (Balasubramanyam et al., 2004; Arif et al., 2009). In contrast, CTPB, an anacardic acid-inspired benzamide, has been reported to function as an activator of p300, but not of PCAF (Souto et al., 2010; Balasubramanyam et al., 2003; Mantelingu et al., 2007). We treated mouse primary mesencephalic cultures with either garcinol (5 μM) or CTPB (10 μM), and then PKCδ immunoreactivity of TH-positive neurons was determined. As shown in Fig. 9*A*, immunocytochemical staining revealed that the level of PKCδ immunoreactivity in TH neurons was dramatically reduced by garcinol exposure, and in contrast, CTPB treatment significantly enhanced PKCδ immunofluorescence. Fluorescent intensity analysis revealed a ~60% ($p<0.01$) decrease and ~170% ($p<0.05$) increase in PKCδ immunoreactivity in garcinol-treated and CTPB-treated TH neurons, respectively (Fig. 9*B*). These results further demonstrated that p300 can

regulate the PKCδ expression in primary dopamine neurons. Taken together with the reduced p300 levels induced by αsyn (Fig. 8), these results suggest that inhibition of p300-mediated transcriptional events by αsyn could contribute to the down-regulation of PKCδ.

Down-regulation of p300 in α-synuclein transgenic mice

Thus far, the *in vitro* experiments indicated that p300 is likely to be the major target molecule of αsyn responsible for the ultimate impingement on the PKCδ transcription. The final step in our study was to verify whether αsyn overexpression down-regulates p300 *in vivo*. To accomplish this, we compared double immunohistochemical labeling of p300 levels within TH positive neurons in the substantia nigra of αsyn transgenic (htg) mice *versus* control (non-tg) animals. As shown in Fig. 10, p300 (stained in red) is predominantly distributed in the nucleus in TH-positive neurons (stained in green). The majority of TH-positive neurons in control mice exhibited significant p300 expression as shown by the intensive p300 immunoreactivity. In contrast, TH-immunoreactive neurons in αsyn transgenic mice showed weak or no immunoreactivity for p300. Taken together with *in vitro* results, these findings in an animal model clearly demonstrate that the suppression of p300 by αsyn contributes to the down-regulation of PKCδ.

Discussion

In the present study, we provide evidence that the normal level of human wild-type αsyn is able to attenuate the MPP^+-induced dopaminergic degeneration by inhibiting the proapoptotic PKCδ gene expression. To our knowledge, this is the first evidence that αsyn is implicated in modulation of PKCδ expression *via* p300. Stable expression of human wild-type αsyn in N27 dopaminergic cells greatly attenuates the MPP^+-induced proteolytic cleavage and nuclear translocation of the PKCδ catalytic fragment, leading to a neuroprotective effect. Conversely, restoring PKCδ expression significantly ablates such neuroprotective function. Additionally, we observed that NFκB and p300 are actively involved in the modulation of PKCδ gene expression in primary dopaminergic neurons. NFκB/p300 inhibition remarkably reduces the extent of PKCδ expression in primary dopaminergic neurons, whereas activation of p300 induces a significantly increased level of PKCδ. Furthermore, we show a dramatically decreased expression of both PKCδ and p300 proteins in dopaminergic neurons in αsyn transgenic mice. In addition, we systematically characterized the mechanism by which αsyn represses PKCδ gene expression. We demonstrated that αsyn does not interfere with PKCδ protein and mRNA turnover but acts *via* direct transcriptional repression. Moreover, we provide evidence linking acetylation events to PKCδ repression mediated by αsyn. First, αsyn inhibits NFκB acetylation, leading to a reduced NFκB transcriptional activity. Second, αsyn disrupts p300 HAT activity. Finally, we show that increasing the cellular acetylation by HDAC inhibitor treatment increases PKCδ expression in an isoform-dependent manner. Collectively, our results support a working model in which αsyn acts to inhibit p300 levels and its HAT activity to repress PKCδ expression and thereby protect against neurotoxicity. These findings might provide mechanistic insights into the physiological role of αsyn in regulating neuronal cell death by suppressing the proapoptotic kinase PKCδ expression. Our proposed model based on the experimental results is illustrated in Scheme 1, in which the inhibition of PKCδ transcription by cytoplasmic αsyn to prevent cell death occurs by disrupting both NFκB and p300 activation, at least as a consequence of the reduced p300 proteins and subsequent decrease in HAT activity.

αSyn is highly abundant in presynaptic terminals of mammalian brain, making up to 0.1% of total brain proteins (Iwai et al., 1995; Sidhu et al., 2004). Although αsyn may have various roles in dopamine synthesis and homeostasis (Perez et al., 2002; Peng et al., 2005b), membrane trafficking (Outeiro and Lindquist, 2003; Cooper et al., 2006), synaptic plasticity

(Clayton and George, 1998; Stephan et al., 2002), and as antioxidant or molecular chaperone (Ostrerova et al., 1999; Zhu et al., 2006), its physiological role is still unclear. Mutations in αsyn gene promote aggregation of αsyn proteins and are linked to PD (Norris et al., 2004). Furthermore, transgenic overexpression of mutant αsyn (A53T) in mice produces neurodegeneration (Giasson et al., 2002; Lee et al., 2002). However, controversy remains about the toxicological properties of wild-type αsyn. Several lines of wild-type αsyn transgenic mice fail to show pathological phenotype (Matsuoka et al., 2001; Rathke-Hartlieb et al., 2001). Furthermore, growing evidence suggests a neuroprotective role for wild-type αsyn. For example, wild-type αsyn, but not its mutant proteins, protects dopaminergic neurons against MPP^+ or rotenone toxicity (Jensen et al., 2003). Transgenic mice overexpressing either the wild-type or the A53T mutant αsyn are resistant to paraquat-induced dopaminergic cell death (Manning-Bog et al., 2003). The transgenic model used in the current study that overexpresses wild-type human αsyn exerts neuroprotection against CSPα-induced neurodegeneration (Chandra et al., 2005). Several hypotheses may explain αsyn-mediated neuroprotection. It is conceivable that αsyn plays a dual role in the nervous system. When expressed at physiological levels, it may function as a normal protein that contributes to cell survival. In contrast, αsyn overexpressed beyond a certain threshold might induce cytotoxicity. A previous study showed that at nanomolar concentrations, αsyn prevented cell death, whereas at both low micromolar and overexpressed levels, αsyn became neurotoxic (Seo et al., 2002). Since the levels of αsyn achieved in our stable N27 cells are within physiological range (Fig. 1*A*), our results support protective functions of this protein. In addition to the extent of αsyn expression, an alternative possibility is that dysregulation of subcellular αsyn may contribute to PD. αSyn exists either in a membrane-bound state that peripherally attaches to vesicles, or in a soluble form that is freely diffusible in the cytoplasm. The translocation between these two subcellular compartments is crucial for the normal function of αsyn (Bennett, 2005; Wislet-Gendebien et al., 2006). Although αsyn was initially recognized as a cytoplasmic protein (Iwai et al., 1995), several lines of evidence have also documented localization of αsyn in the nucleus (Goers et al., 2003; Zhang et al., 2008). Interestingly, a previous study indicated that nuclear αsyn promoted neurotoxicity, and conversely, cytoplasmic localization of αsyn was neuroprotective (Kontopoulos et al., 2006). In the present study, the cytoplasmic localization of αsyn that prevented MPP^+-induced cell death partially confirmed this finding (Fig. 2). Additionally, αsyn has been shown to function as a negative mediator of DA synthesis *via* interactions with TH and/or PP2A to inhibit TH activity (Perez et al., 2002; Peng et al., 2005b). We also reported that PKCδ negatively regulates TH activity by binding and phosphorylating PP2A (Zhang et al., 2007c). In the present study, we demonstrated that αsyn represses PKCδ transcription, suggesting that αsyn-mediated repression of PKCδ may alter DA synthesis. Importantly, we found a reduced PKCδ expression in αsyn transgenic mouse models, indicating the αsyn overexpression represses the proapoptotic kinase PKCδ *in vivo*. These results may explain why αsyn overexpressing mice are resistant to neurodegeneration in dopaminergic neurons despite the high accumulation of the protein in the substantia nigra.

Although our results indicate that p300 pathway is likely the major pathway controlling the down-regulation of PKCδ in transgenic animal, it is possible that other PKCδ downregulation mechanisms come into play, acting alone or in concert, since overexpression of αsyn was found to significantly alter multiple signaling pathways, including stress response, transcription factors, apoptosis-inducing molecules, and membrane-bound proteins (Baptista et al., 2003). Moreover, αsyn has been shown to be able to directly associate with histones and inhibit histone acetylation, suggesting a direct role of the protein in regulation of gene transcription (Goers et al., 2003; Kontopoulos et al., 2006).

We report here for the first time the repression of the PKCδ gene by αsyn in dopaminergic neurons mediated through the transcription factors NFκB and p300. Our results show that

αsyn inhibits NFκB transcriptional activity at the level of p65 acetylation, without affecting NFκB/IκBα nuclear translocation, IκBα degradation, or NFκB/IκBα protein levels. It should be noted, however, that acetylation of p65 to mediate NFκB transcriptional activity may be more complex, as acetylation of discrete lysine sites may regulate different nuclear functions (Chen et al., 2002). Independent of regulation of p65 acetylation levels, modulation of p300/CBP-mediated acetylation of p50 has to be considered as one mechanism for the inhibition of p50 binding activity (Fig. 5*D*) by αsyn, because acetylation of p50 increases its DNA binding and further induces NFκB transcriptional activity (Deng et al., 2003). Moreover, analysis of the PKCδ promoter has uncovered multiple potential transcription factor sites. Therefore, it is also possible that one or more of those factors may contribute to the attenuation of PKCδ expression by αsyn.

An important finding of this study is that αsyn specifically decreases p300 protein *in vivo* and *in vitro*. Our model introduces loss of p300 as an underlying mechanism of its reduced HAT activity. p300 appears to play at least two major roles in αsyn-mediated suppression of PKCδ. First, loss of p300 proteins and its corresponding HAT activity reduces p65 acetylation and binding activity to PKCδ promoter, thereby resulting in downregulation of PKCδ. Second, PKCδ gene expression itself may be dependent on p300. Thus, the depletion of p300 proteins would decrease the recruitment and binding of p300 onto PKCδ promoter, and subsequently may interfere with the interactions between p300 and NFκB or other transcriptional complexes, eventually blocking PKCδ transcription. However, the mechanism by which αsyn disrupts the p300 protein is unclear. Our unpublished data indicate that αsyn does not likely regulate p300 protein level at the transcriptional level. Further investigation should reveal whether αsyn inhibits p300 protein by an alternative mechanism, such as degradation mediated by proteasome as reported previously (Poizat et al., 2005).

It is important to note that regulation of acetylation of p65 could not be limited to the acetyltransferase activities of p300 and CBP because deacetylation reactions can also influence the overall acetylation status of NFκB. In fact, it has been reported that p65 is reversibly acetylated by p300 and CBP and subsequently deacetylated by HDACs, most notably, HDAC3 (Kiernan et al., 2003). Therefore, the contribution of HDACs to the inhibition of p65 acetylation by αsyn remains to be elucidated. In addition to acetylation, p65 is also regulated by the modification of phosphorylation, which can potentiate the transcription by enhancing p65 association with the p300/CBP coactivator (Zhong et al., 2002). The influence of αsyn on NFκB transactivation by alteration of p65 phosphorylation status is yet to be determined.

In summary, our results are based on multiple independent techniques that together elucidate the molecular and cellular mechanisms underlying the down-regulation of PKCδ by αsyn. These findings expand the role of αsyn in neuroprotection and have important implications for the development of novel drug therapies for PD.

Supplementary Material

Refer to Web version on PubMed Central for supplementary material.

Acknowledgments

This work was supported by National Institutes of Health Grants NS38644 (AGK), NS65167 (AK) and ES10586 (AGK). The W. Eugene and Linda Lloyd Endowed Chair to AGK is also acknowledged. We thank MaryAnn deVries for assistance in the preparation of this manuscript.

References

Albani D, Peverelli E, Rametta R, Batelli S, Veschini L, Negro A, Forloni G. Protective effect of TAT-delivered alpha-synuclein: relevance of the C-terminal domain and involvement of HSP70. Faseb J 2004;18:1713–1715. [PubMed: 15345691]

Alves Da Costa C, Paitel E, Vincent B, Checler F. Alpha-synuclein lowers p53-dependent apoptotic response of neuronal cells. Abolishment by 6-hydroxydopamine and implication for Parkinson's disease. J Biol Chem 2002;277:50980–50984. [PubMed: 12397073]

Anantharam V, Kitazawa M, Wagner J, Kaul S, Kanthasamy AG. Caspase-3-dependent proteolytic cleavage of protein kinase Cdelta is essential for oxidative stress-mediated dopaminergic cell death after exposure to methylcyclopentadienyl manganese tricarbonyl. J Neurosci 2002;22:1738–1751. [PubMed: 11880503]

Andra K, Abramowski D, Duke M, Probst A, Wiederhold KH, Burki K, Goedert M, Sommer B, Staufenbiel M. Expression of APP in transgenic mice: a comparison of neuron-specific promoters. Neurobiol Aging 1996;17:183–190. [PubMed: 8744399]

Arif M, Pradhan SK, Thanuja GR, Vedamurthy BM, Agrawal S, Dasgupta D, Kundu TK. Mechanism of p300 specific histone acetyltransferase inhibition by small molecules. J Med Chem 2009;52:267–277. [PubMed: 19086895]

Balasubramanyam K, Swaminathan V, Ranganathan A, Kundu TK. Small molecule modulators of histone acetyltransferase p300. J Biol Chem 2003;278:19134–19140. [PubMed: 12624111]

Balasubramanyam K, Altaf M, Varier RA, Swaminathan V, Ravindran A, Sadhale PP, Kundu TK. Polyisoprenylated benzophenone, garcinol, a natural histone acetyltransferase inhibitor, represses chromatin transcription and alters global gene expression. J Biol Chem 2004;279:33716–33726. [PubMed: 15155757]

Baptista MJ, O'Farrell C, Daya S, Ahmad R, Miller DW, Hardy J, Farrer MJ, Cookson MR. Co-ordinate transcriptional regulation of dopamine synthesis genes by alpha-synuclein in human neuroblastoma cell lines. J Neurochem 2003;85:957–968. [PubMed: 12716427]

Bennett MC. The role of alpha-synuclein in neurodegenerative diseases. Pharmacol Ther 2005;105:311–331. [PubMed: 15737408]

Brodie C, Blumberg PM. Regulation of cell apoptosis by protein kinase c delta. Apoptosis 2003;8:19–27. [PubMed: 12510148]

Burke RE. Programmed cell death and new discoveries in the genetics of parkinsonism. J Neurochem 2008;104:875–890. [PubMed: 17996022]

Cartharius K, Frech K, Grote K, Klocke B, Haltmeier M, Klingenhoff A, Frisch M, Bayerlein M, Werner T. MatInspector and beyond: promoter analysis based on transcription factor binding sites. Bioinformatics 2005;21:2933–2942. [PubMed: 15860560]

Chan HM, La Thangue NB. p300/CBP proteins: HATs for transcriptional bridges and scaffolds. J Cell Sci 2001;114:2363–2373. [PubMed: 11559745]

Chandra S, Gallardo G, Fernandez-Chacon R, Schluter OM, Sudhof TC. Alpha-synuclein cooperates with CSPalpha in preventing neurodegeneration. Cell 2005;123:383–396. [PubMed: 16269331]

Chen L, Fischle W, Verdin E, Greene WC. Duration of nuclear NF-kappaB action regulated by reversible acetylation. Science 2001;293:1653–1657. [PubMed: 11533489]

Chen LF, Mu Y, Greene WC. Acetylation of RelA at discrete sites regulates distinct nuclear functions of NF-kappaB. Embo J 2002;21:6539–6548. [PubMed: 12456660]

Chen YL, Law PY, Loh HH. Sustained activation of phosphatidylinositol 3-kinase/Akt/nuclear factor kappaB signaling mediates G protein-coupled delta-opioid receptor gene expression. J Biol Chem 2006;281:3067–3074. [PubMed: 16316997]

Clarkson ED, Edwards-Prasad J, Freed CR, Prasad KN. Immortalized dopamine neurons: A model to study neurotoxicity and neuroprotection. Proc Soc Exp Biol Med 1999;222:157–163. [PubMed: 10564540]

Clayton DF, George JM. The synucleins: a family of proteins involved in synaptic function, plasticity, neurodegeneration and disease. Trends Neurosci 1998;21:249–254. [PubMed: 9641537]

Cooper AA, Gitler AD, Cashikar A, Haynes CM, Hill KJ, Bhullar B, Liu K, Xu K, Strathearn KE, Liu F, Cao S, Caldwell KA, Caldwell GA, Marsischky G, Kolodner RD, Labaer J, Rochet JC, Bonini

NM, Lindquist S. Alpha-synuclein blocks ER-Golgi traffic and Rab1 rescues neuron loss in Parkinson's models. Science 2006;313:324–328. [PubMed: 16794039]

Dauer W, Przedborski S. Parkinson's disease: mechanisms and models. Neuron 2003;39:889–909. [PubMed: 12971891]

de Erausquin GA, Hyrc K, Dorsey DA, Mamah D, Dokucu M, Masco DH, Walton T, Dikranian K, Soriano M, Garcia Verdugo JM, Goldberg MP, Dugan LL. Nuclear translocation of nuclear transcription factor-kappa B by alpha-amino-3-hydroxy-5-methyl-4-isoxazolepropionic acid receptors leads to transcription of p53 and cell death in dopaminergic neurons. Mol Pharmacol 2003;63:784–790. [PubMed: 12644578]

Deng WG, Zhu Y, Wu KK. Up-regulation of p300 binding and p50 acetylation in tumor necrosis factor-alpha-induced cyclooxygenase-2 promoter activation. J Biol Chem 2003;278:4770–4777. [PubMed: 12471036]

DeVries TA, Neville MC, Reyland ME. Nuclear import of PKCdelta is required for apoptosis: identification of a novel nuclear import sequence. Embo J 2002;21:6050–6060. [PubMed: 12426377]

Duan J, Friedman J, Nottingham L, Chen Z, Ara G, Van Waes C. Nuclear factor-kappaB p65 small interfering RNA or proteasome inhibitor bortezomib sensitizes head and neck squamous cell carcinomas to classic histone deacetylase inhibitors and novel histone deacetylase inhibitor PXD101. Mol Cancer Ther 2007;6:37–50. [PubMed: 17237265]

Ghosh A, Chandran K, Kalivendi SV, Joseph J, Antholine WE, Hillard CJ, Kanthasamy A, Kanthasamy A, Kalyanaraman B. Neuroprotection by a mitochondria-targeted drug in a Parkinson's disease model. Free Radic Biol Med. 2010

Giasson BI, Duda JE, Quinn SM, Zhang B, Trojanowski JQ, Lee VM. Neuronal alpha-synucleinopathy with severe movement disorder in mice expressing A53T human alpha-synuclein. Neuron 2002;34:521–533. [PubMed: 12062037]

Goers J, Manning-Bog AB, McCormack AL, Millett IS, Doniach S, Di Monte DA, Uversky VN, Fink AL. Nuclear localization of alpha-synuclein and its interaction with histones. Biochemistry 2003;42:8465–8471. [PubMed: 12859192]

Greenamyre JT, Hastings TG. Biomedicine. Parkinson's--divergent causes, convergent mechanisms. Science 2004;304:1120–1122. [PubMed: 15155938]

Gustin JA, Ozes ON, Akca H, Pincheira R, Mayo LD, Li Q, Guzman JR, Korgaonkar CK, Donner DB. Cell type-specific expression of the IkappaB kinases determines the significance of phosphatidylinositol 3-kinase/Akt signaling to NF-kappa B activation. J Biol Chem 2004;279:1615–1620. [PubMed: 14585846]

Hashimoto M, Hsu LJ, Rockenstein E, Takenouchi T, Mallory M, Masliah E. alpha-Synuclein protects against oxidative stress via inactivation of the c-Jun N-terminal kinase stress-signaling pathway in neuronal cells. J Biol Chem 2002;277:11465–11472. [PubMed: 11790792]

Hatcher JM, Pennell KD, Miller GW. Parkinson's disease and pesticides: a toxicological perspective. Trends Pharmacol Sci 2008;29:322–329. [PubMed: 18453001]

Iwai A, Masliah E, Yoshimoto M, Ge N, Flanagan L, de Silva HA, Kittel A, Saitoh T. The precursor protein of non-A beta component of Alzheimer's disease amyloid is a presynaptic protein of the central nervous system. Neuron 1995;14:467–475. [PubMed: 7857654]

Jensen PJ, Alter BJ, O'Malley KL. Alpha-synuclein protects naive but not dbcAMP-treated dopaminergic cell types from 1-methyl-4-phenylpyridinium toxicity. J Neurochem 2003;86:196–209. [PubMed: 12807439]

Jing Q, Huang S, Guth S, Zarubin T, Motoyama A, Chen J, Di Padova F, Lin SC, Gram H, Han J. Involvement of microRNA in AU-rich element-mediated mRNA instability. Cell 2005;120:623–634. [PubMed: 15766526]

Kanthasamy AG, Kitazawa M, Kanthasamy A, Anantharam V. Role of proteolytic activation of protein kinase Cdelta in oxidative stress-induced apoptosis. Antioxid Redox Signal 2003;5:609–620. [PubMed: 14580317]

Kanthasamy AG, Anantharam V, Zhang D, Latchoumycandane C, Jin H, Kaul S, Kanthasamy A. A novel peptide inhibitor targeted to caspase-3 cleavage site of a proapoptotic kinase protein kinase

C delta (PKCdelta) protects against dopaminergic neuronal degeneration in Parkinson's disease models. Free Radic Biol Med 2006;41:1578–1589. [PubMed: 17045926]

Kaul S, Anantharam V, Kanthasamy A, Kanthasamy AG. Wild-type alpha-synuclein interacts with pro-apoptotic proteins PKCdelta and BAD to protect dopaminergic neuronal cells against MPP+-induced apoptotic cell death. Brain Res Mol Brain Res 2005a;139:137–152. [PubMed: 15978696]

Kaul S, Kanthasamy A, Kitazawa M, Anantharam V, Kanthasamy AG. Caspase-3 dependent proteolytic activation of protein kinase C delta mediates and regulates 1-methyl-4-phenylpyridinium (MPP+)-induced apoptotic cell death in dopaminergic cells: relevance to oxidative stress in dopaminergic degeneration. Eur J Neurosci 2003;18:1387–1401. [PubMed: 14511319]

Kaul S, Anantharam V, Yang Y, Choi CJ, Kanthasamy A, Kanthasamy AG. Tyrosine phosphorylation regulates the proteolytic activation of protein kinase Cdelta in dopaminergic neuronal cells. J Biol Chem 2005b;280:28721–28730. [PubMed: 15961393]

Kiernan R, Bres V, Ng RW, Coudart MP, El Messaoudi S, Sardet C, Jin DY, Emiliani S, Benkirane M. Post-activation turn-off of NF-kappa B-dependent transcription is regulated by acetylation of p65. J Biol Chem 2003;278:2758–2766. [PubMed: 12419806]

Kitazawa M, Anantharam V, Kanthasamy AG. Dieldrin induces apoptosis by promoting caspase-3-dependent proteolytic cleavage of protein kinase Cdelta in dopaminergic cells: relevance to oxidative stress and dopaminergic degeneration. Neuroscience 2003;119:945–964. [PubMed: 12831855]

Kitazawa M, Anantharam V, Yang Y, Hirata Y, Kanthasamy A, Kanthasamy AG. Activation of protein kinase C delta by proteolytic cleavage contributes to manganese-induced apoptosis in dopaminergic cells: protective role of Bcl-2. Biochem Pharmacol 2005;69:133–146. [PubMed: 15588722]

Kontopoulos E, Parvin JD, Feany MB. Alpha-synuclein acts in the nucleus to inhibit histone acetylation and promote neurotoxicity. Hum Mol Genet 2006;15:3012–3023. [PubMed: 16959795]

Latchoumycandane C, Anantharam V, Kitazawa M, Yang Y, Kanthasamy A, Kanthasamy AG. Protein kinase Cdelta is a key downstream mediator of manganese-induced apoptosis in dopaminergic neuronal cells. J Pharmacol Exp Ther 2005;313:46–55. [PubMed: 15608081]

Lee DW, Rajagopalan S, Siddiq A, Gwiazda R, Yang L, Beal Beal, Ratan RR, Andersen JK. Inhibition of prolyl hydroxylase protects against 1-methyl-4-phenyl-1,2,3,6-tetrahydropyridine-induced neurotoxicity: model for the potential involvement of the hypoxia-inducible factor pathway in Parkinson disease. J Biol Chem 2009;284:29065–29076. [PubMed: 19679656]

Lee MK, Stirling W, Xu Y, Xu X, Qui D, Mandir AS, Dawson TM, Copeland NG, Jenkins NA, Price DL. Human alpha-synuclein-harboring familial Parkinson's disease-linked Ala-53 --> Thr mutation causes neurodegenerative disease with alpha-synuclein aggregation in transgenic mice. Proc Natl Acad Sci U S A 2002;99:8968–8973. [PubMed: 12084935]

Leng Y, Chuang DM. Endogenous alpha-synuclein is induced by valproic acid through histone deacetylase inhibition and participates in neuroprotection against glutamate-induced excitotoxicity. J Neurosci 2006;26:7502–7512. [PubMed: 16837598]

Li LC, Dahiya R. MethPrimer: designing primers for methylation PCRs. Bioinformatics 2002;18:1427–1431. [PubMed: 12424112]

Manning-Bog AB, McCormack AL, Purisai MG, Bolin LM, Di Monte DA. Alpha-synuclein overexpression protects against paraquat-induced neurodegeneration. J Neurosci 2003;23:3095–3099. [PubMed: 12716914]

Mantelingu K, Kishore AH, Balasubramanyam K, Kumar GV, Altaf M, Swamy SN, Selvi R, Das C, Narayana C, Rangappa KS, Kundu TK. Activation of p300 histone acetyltransferase by small molecules altering enzyme structure: probed by surface-enhanced Raman spectroscopy. J Phys Chem B 2007;111:4527–4534. [PubMed: 17417897]

Matsuoka Y, Vila M, Lincoln S, McCormack A, Picciano M, LaFrancois J, Yu X, Dickson D, Langston WJ, McGowan E, Farrer M, Hardy J, Duff K, Przedborski S, Di Monte DA. Lack of nigral pathology in transgenic mice expressing human alpha-synuclein driven by the tyrosine hydroxylase promoter. Neurobiol Dis 2001;8:535–539. [PubMed: 11442360]

Monti B, Polazzi E, Batti L, Crochemore C, Virgili M, Contestabile A. Alpha-synuclein protects cerebellar granule neurons against 6-hydroxydopamine-induced death. J Neurochem 2007;103:518–530. [PubMed: 17635667]

Morgenstern B, Dress A, Werner T. Multiple DNA and protein sequence alignment based on segment-to-segment comparison. Proc Natl Acad Sci U S A 1996;93:12098–12103. [PubMed: 8901539]

Morgenstern B, Frech K, Dress A, Werner T. DIALIGN: finding local similarities by multiple sequence alignment. Bioinformatics 1998;14:290–294. [PubMed: 9614273]

Nakatani F, Tanaka K, Sakimura R, Matsumoto Y, Matsunobu T, Li X, Hanada M, Okada T, Iwamoto Y. Identification of p21WAF1/CIP1 as a direct target of EWS-Fli1 oncogenic fusion protein. J Biol Chem 2003;278:15105–15115. [PubMed: 12560328]

Norris EH, Giasson BI, Lee VM. Alpha-synuclein: normal function and role in neurodegenerative diseases. Curr Top Dev Biol 2004;60:17–54. [PubMed: 15094295]

Ostrerova N, Petrucelli L, Farrer M, Mehta N, Choi P, Hardy J, Wolozin B. alpha-Synuclein shares physical and functional homology with 14-3-3 proteins. J Neurosci 1999;19:5782–5791. [PubMed: 10407019]

Outeiro TF, Lindquist S. Yeast cells provide insight into alpha-synuclein biology and pathobiology. Science 2003;302:1772–1775. [PubMed: 14657500]

Patrone G, Puppo F, Cusano R, Scaranari M, Ceccherini I, Puliti A, Ravazzolo R. Nuclear run-on assay using biotin labeling, magnetic bead capture and analysis by fluorescence-based RT-PCR. Biotechniques 2000;29:1012–1014. 1016–1017. [PubMed: 11084863]

Peng J, Stevenson FF, Doctrow SR, Andersen JK. Superoxide dismutase/catalase mimetics are neuroprotective against selective paraquat-mediated dopaminergic neuron death in the substantial nigra: implications for Parkinson disease. J Biol Chem 2005a;280:29194–29198. [PubMed: 15946937]

Peng X, Tehranian R, Dietrich P, Stefanis L, Perez RG. Alpha-synuclein activation of protein phosphatase 2A reduces tyrosine hydroxylase phosphorylation in dopaminergic cells. J Cell Sci 2005b;118:3523–3530. [PubMed: 16030137]

Perez RG, Waymire JC, Lin E, Liu JJ, Guo F, Zigmond MJ. A role for alpha-synuclein in the regulation of dopamine biosynthesis. J Neurosci 2002;22:3090–3099. [PubMed: 11943812]

Poizat C, Puri PL, Bai Y, Kedes L. Phosphorylation-dependent degradation of p300 by doxorubicin-activated p38 mitogen-activated protein kinase in cardiac cells. Mol Cell Biol 2005;25:2673–2687. [PubMed: 15767673]

Rathke-Hartlieb S, Kahle PJ, Neumann M, Ozmen L, Haid S, Okochi M, Haass C, Schulz JB. Sensitivity to MPTP is not increased in Parkinson's disease-associated mutant alpha-synuclein transgenic mice. J Neurochem 2001;77:1181–1184. [PubMed: 11359883]

Seo JH, Rah JC, Choi SH, Shin JK, Min K, Kim HS, Park CH, Kim S, Kim EM, Lee SH, Lee S, Suh SW, Suh YH. Alpha-synuclein regulates neuronal survival via Bcl-2 family expression and PI3/Akt kinase pathway. Faseb J 2002;16:1826–1828. [PubMed: 12223445]

Sidhu A, Wersinger C, Moussa CE, Vernier P. The role of alpha-synuclein in both neuroprotection and neurodegeneration. Ann N Y Acad Sci 2004;1035:250–270. [PubMed: 15681812]

Souto JA, Benedetti R, Otto K, Miceli M, Alvarez R, Altucci L, de Lera AR. New anacardic acid-inspired benzamides: histone lysine acetyltransferase activators. ChemMedChem 2010;5:1530–1540. [PubMed: 20683922]

Spillantini MG, Crowther RA, Jakes R, Hasegawa M, Goedert M. alpha-Synuclein in filamentous inclusions of Lewy bodies from Parkinson's disease and dementia with lewy bodies. Proc Natl Acad Sci U S A 1998;95:6469–6473. [PubMed: 9600990]

Stephan A, Davis S, Salin H, Dumas S, Mallet J, Laroche S. Age-dependent differential regulation of genes encoding APP and alpha-synuclein in hippocampal synaptic plasticity. Hippocampus 2002;12:55–62. [PubMed: 11918289]

Suh KS, Tatunchak TT, Crutchley JM, Edwards LE, Marin KG, Yuspa SH. Genomic structure and promoter analysis of PKC-delta. Genomics 2003;82:57–67. [PubMed: 12809676]

Takai D, Jones PA. Comprehensive analysis of CpG islands in human chromosomes 21 and 22. Proc Natl Acad Sci U S A 2002;99:3740–3745. [PubMed: 11891299]

Wislet-Gendebien S, D'Souza C, Kawarai T, St George-Hyslop P, Westaway D, Fraser P, Tandon A. Cytosolic proteins regulate alpha-synuclein dissociation from presynaptic membranes. J Biol Chem 2006;281:32148–32155. [PubMed: 16926154]

Yang Y, Kaul S, Zhang D, Anantharam V, Kanthasamy AG. Suppression of caspase-3-dependent proteolytic activation of protein kinase C delta by small interfering RNA prevents MPP+-induced dopaminergic degeneration. Mol Cell Neurosci 2004;25:406–421. [PubMed: 15033169]

Zafar KS, Inayat-Hussain SH, Ross D. A comparative study of proteasomal inhibition and apoptosis induced in N27 mesencephalic cells by dopamine and MG132. J Neurochem 2007;102:913–921. [PubMed: 17504267]

Zhang D, Anantharam V, Kanthasamy A, Kanthasamy AG. Neuroprotective effect of protein kinase C delta inhibitor rottlerin in cell culture and animal models of Parkinson's disease. J Pharmacol Exp Ther 2007a;322:913–922. [PubMed: 17565007]

Zhang D, Kanthasamy A, Yang Y, Anantharam V, Kanthasamy A. Protein kinase C delta negatively regulates tyrosine hydroxylase activity and dopamine synthesis by enhancing protein phosphatase-2A activity in dopaminergic neurons. J Neurosci 2007b;27:5349–5362. [PubMed: 17507557]

Zhang D, Kanthasamy A, Yang Y, Anantharam V, Kanthasamy A. Protein kinase Cdelta negatively regulates tyrosine hydroxylase activity and dopamine synthesis by enhancing protein phosphatase-2A activity in dopaminergic neurons. J Neurosci 2007c;27:5349–5362. [PubMed: 17507557]

Zhang L, Zhang C, Zhu Y, Cai Q, Chan P, Ueda K, Yu S, Yang H. Semi-quantitative analysis of alpha-synuclein in subcellular pools of rat brain neurons: an immunogold electron microscopic study using a C-terminal specific monoclonal antibody. Brain Res 2008;1244:40–52. [PubMed: 18817762]

Zhong H, May MJ, Jimi E, Ghosh S. The phosphorylation status of nuclear NF-kappa B determines its association with CBP/p300 or HDAC-1. Mol Cell 2002;9:625–636. [PubMed: 11931769]

Zhou C, Huang Y, Przedborski S. Oxidative stress in Parkinson's disease: a mechanism of pathogenic and therapeutic significance. Ann N Y Acad Sci 2008;1147:93–104. [PubMed: 19076434]

Zhu M, Qin ZJ, Hu D, Munishkina LA, Fink AL. Alpha-synuclein can function as an antioxidant preventing oxidation of unsaturated lipid in vesicles. Biochemistry 2006;45:8135–8142. [PubMed: 16800638]

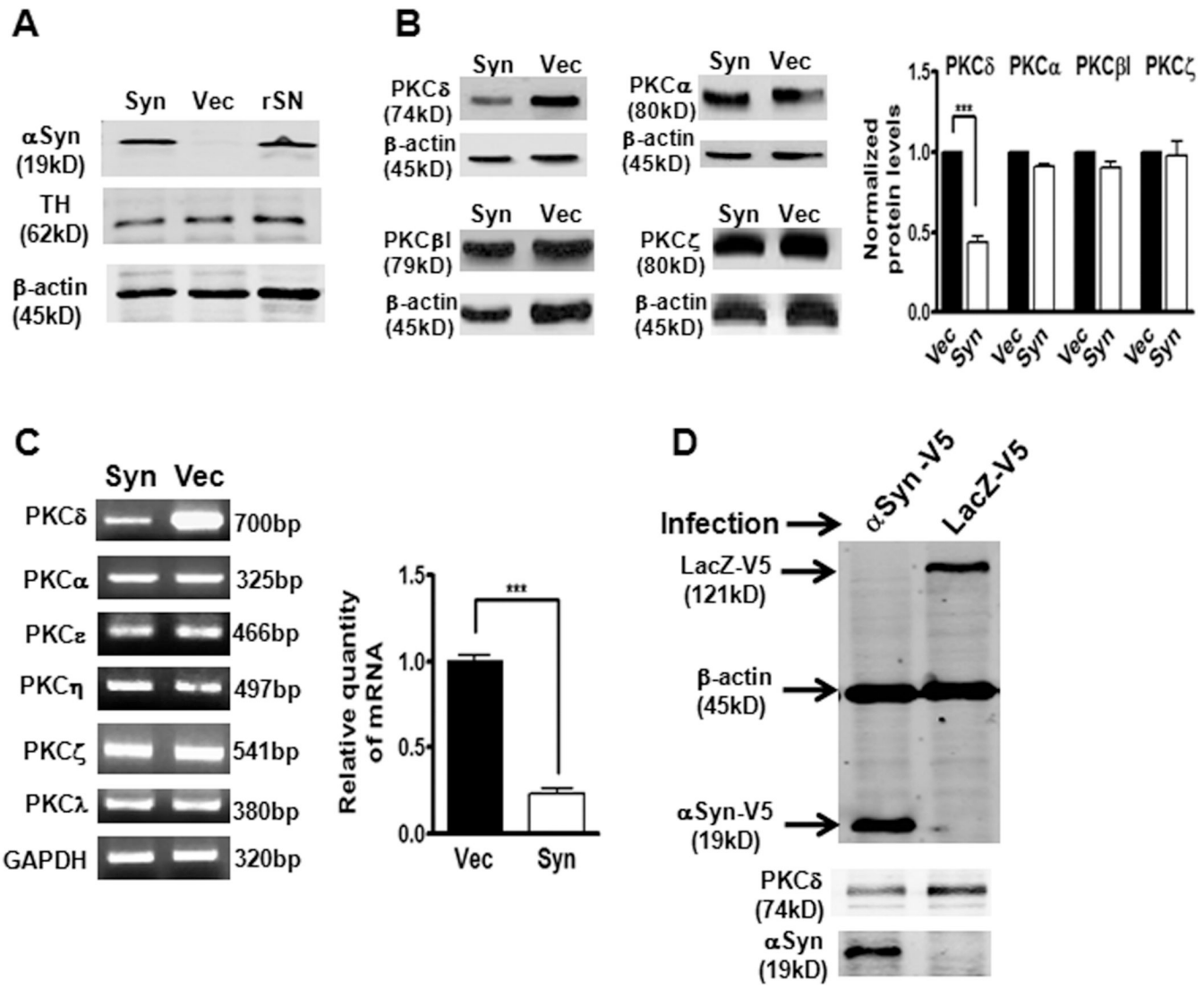

Figure 1.

α-Synuclein specifically down-regulates PKCδ isoform in N27 dopaminergic cells. ***A***, Whole cell extracts from stably expressing αsyn N27 cells (Syn), vector control N27 cells (Vec), and rat substantia nigra brain (rSN) were prepared. Expression of αsyn and TH were determined by immunoblotting assay with antibodies against αsyn (Syn-1, BD Biosciences) and TH. β-actin was used as a loading control. ***B***, The specific downregulation of PKCδ protein in αsyn-expressing N27 cells. Representative immunoblots (left panel) and quantitation (right panel) of PKC isoforms (δ, α, βI, and ζ) in whole cell lysates in αsyn-expressing (Syn) and vector control (Vec) N27 cells. Data shown are mean ± SEM from three separate experiments (***$p<0.001$). ***C***, Left: semiquantitative RT-PCR analysis of mRNA levels of various PKC isoforms. Amplicon base pairs (bp) are shown at the right sides of the panel. GAPDH was used as loading control. Right: qRT-PCR analysis for PKCδ mRNA expression in αsyn-expressing and vector control N27 cells. Data shown represent mean ± SEM from four separate experiments preformed in triplicate (***$p<0.001$). ***D***, Transient overexpression of human wild-type αsyn in N27 cells by lentiviral infection down-regulates PKCδ protein expression. N27 cells were infected with lentiviruses expressing LacZ-V5 (control lentiviral vector) or αsyn-V5 for 48 h, and whole cell lysates were

analyzed for V5 and β-actin (top panel), PKCδ (middle panel), and αsyn (bottom panel). A representative immunoblot is shown.

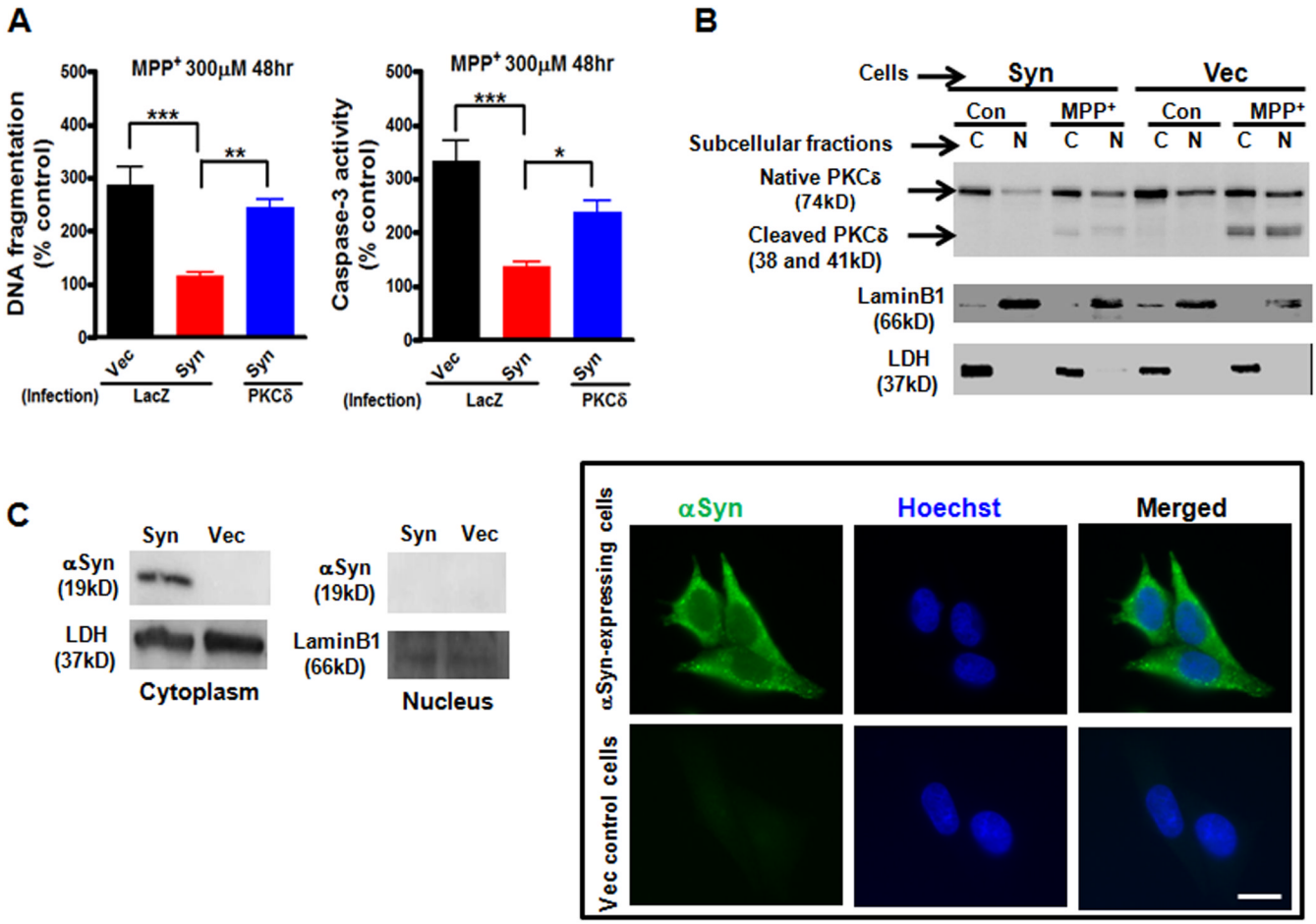

Figure 2.

Deregulation of PKCδ by α-synuclein protects against MPP^+-induced cell death in dopaminergic N27 cells. ***A***, Effects of downregulation of PKCδ by αsyn on MPP^+-induced cell death in dopaminergic N27 cells. αSyn-expressing (Syn) and vector control (Vec) N27 cells were infected with lentiviruses expressing LacZ-V5 or PKCδ-V5 for 24 h. The cells were then exposed to MPP^+ (300μM) for 48 h. Cells were collected and assayed for DNA fragmentation (left panel) and caspase-3 activity (right panel). Data shown represent mean ± SEM from two independent experiments performed in quadruplicate (*p<0.05; **p<0.01; and ***p<0.001). ***B***, MPP^+-induced PKCδ proteolytic cleavage and its nuclear translocation were significantly diminished in αsyn-expressing N27 cells. αSyn-expressing (Syn) and vector control (Vec) N27 cells were exposed to MPP^+ (300 μM) for 36 h. Cytoplasmic (C) and nuclear (N) fractions were prepared for immunoblotting analysis of PKCδ. LDH (cytoplasmic fraction) and Lamin B1 (nuclear fraction) were used as loading controls. ***C***, Cytoplasmic localization of αsyn in αsyn-expressing N27 cells was not affected by MPP^+ treatment. αSyn-expressing (Syn) and vector control (Vec) N27 cells were exposed to MPP^+ (300 μM) for 36 h. Cells were either collected for preparation of cytoplasmic and nuclear extracts and immunoblotting analysis of αsyn (left panel) or stained and visualized under a Nikon TE2000 fluorescence microscope (right panel). Scale bar, 10μm. A representative immunoblot and image of αsyn immunostaining (green) and Hoechst staining (blue) are shown.

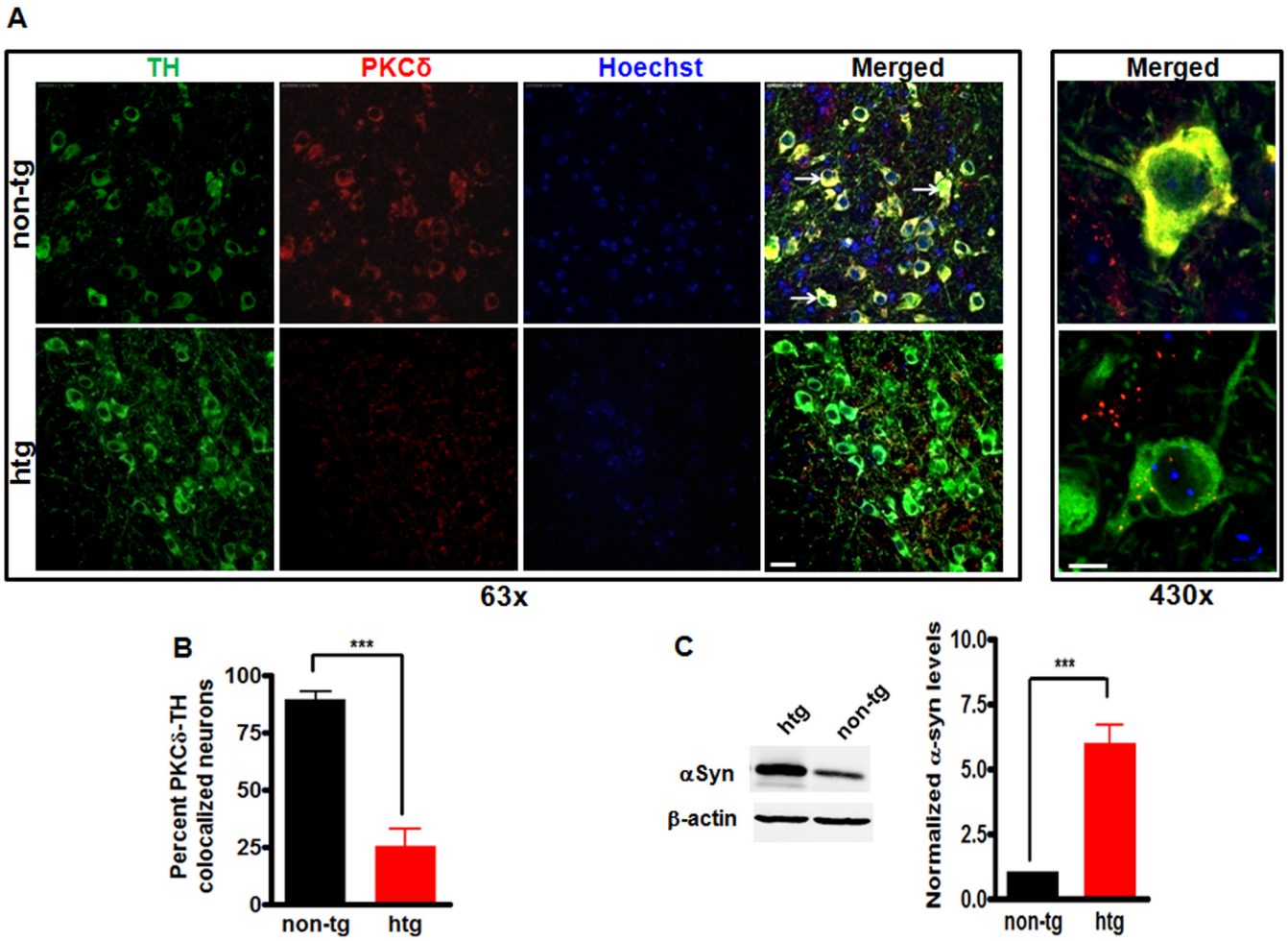

Figure 3.

Decreased PKCδ expression in nigral dopaminergic neurons in α-synuclein overexpressing mice. ***A***, Representative images of immunohistochemical analysis of PKCδ expression within nigral TH-positive neurons. Substantia nigra sections from non-transgenic control (non-tg) mice and αsyn transgenic mice (htg) were stained with PKCδ polyclonal antibody (1:250 dilution) and TH monoclonal antibody (1:1800 dilution), followed by incubation with Alexa 568-conjugated (red; 1:1000) and Alexa 488-conjuated (green; 1:1000) secondary antibodies. Hoechst 33342 (10 μg/ml) was added to stain the nucleus. Confocal images were obtained using a Leica SP5 X confocal microscope system. Green, TH; red, PKCδ; blue, nucleus. White arrows point to dopaminergic neurons with significant PKCδ staining. Scale bar, 25μm (left panel) and 7.5μm (right panel). Magnifications 63× (left panel) and 430× (right panel). ***B***, Quantification of the number of TH neurons containing colocalized PKCδ immunoreactivity was determined by blindly counting 6 fields and averaging. Values expressed as percent of total TH neurons were mean ± SEM and representative for results obtained with three pairs of 6–8-week-old mice (***$p<0.001$). ***C***, To analyze the levels of αsyn in substantial nigra homogenates from transgenic mice overexpressing human wild-type αsyn and non-transgenic mice, substantial nigra homogenates were prepared from transgenic mice (htg) and non-transgenic mice (non-tg) and subjected to immunoblotting analysis of αsyn, and β-actin. Representative immunoblot (left panel) and quantitation (right panel) of αsyn expression were shown. About 6-fold increase in αsyn expression in

substantial nigra was found in transgenic mice. Data were shown as mean ± SEM; n=6 (***p<0.001).

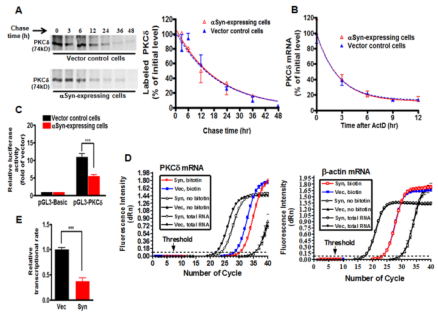

Figure 4.

α-Synuclein suppresses PKCδ transcription without affecting PKCδ protein or mRNA stability in N27 dopaminergic cells. ***A***, Left: Pulse-chase analysis of stability of PKCδ protein. αSyn-expressing and vector control N27 cells were labeled with ^{35}S-methionine, and PKCδ protein was analyzed over 48 h as described in Materials and Methods. Right: The bands were quantified and expressed as percentage of amount present at time 0 h. The data plotted were fit to a one-phase exponential decay model using the nonlinear regression analysis program of Prism 4.0 software as follows: $Y = \text{Span } e^{-Kt} + \text{Plateau}$, where Y starts at Span + Plateau and decays with a rate constant K. The half-life of the protein was determined by 0.693/K. The square of the correlation coefficient (R^2) is used as a measure of goodness-of-fit in regression analysis. Values are mean ± SEM of two independent experiments. ***B***, The stability of PKCδ mRNA was not decreased in αsyn-expressing N27 cells. After treatment with actinomycin D (ActD), total RNA was extracted for qRT-PCR analysis at selected time intervals. The relative abundance of PKCδ mRNA was expressed as a percentage of that present at time 0 h, and data plotted were fit to the one-phase exponential decay model. Values are mean ± SEM of three independent experiments performed in triplicate. ***C***, The PKCδ promoter activation was attenuated in αsyn-expressing cells in reporter assays. Reporter pGL3-PKCδ carrying the PKCδ promoter or pGL3-Basic empty vector was transiently transfected into αsyn-expressing and vector control cells. Cells were collected 24 h post-transfection and assayed for luciferase activity and β-galactosidase activity. Data were normalized and expressed as fold-induction over the pGL3-Basic vector. Values are shown as mean ± SEM of three independent experiments performed in triplicate (***$p<0.001$). ***D***, The relative transcription efficiency of PKCδ was examined by quantitative nuclear run-on assay. Representative amplification plots for PKCδ mRNA (left panel) and β-actin mRNA (right panel) are shown. The change in fluorescence intensity (ΔRn) was plotted on the Y axis. The arrow shows the threshold (dashed lines). ***E***, Quantitation of transcription efficiency. Data are expressed as fold-change in the level of nascent run-on PKCδ mRNA in vector control cells, and are shown as mean ± SEM of three independent experiments performed in triplicate (***$p<0.001$).

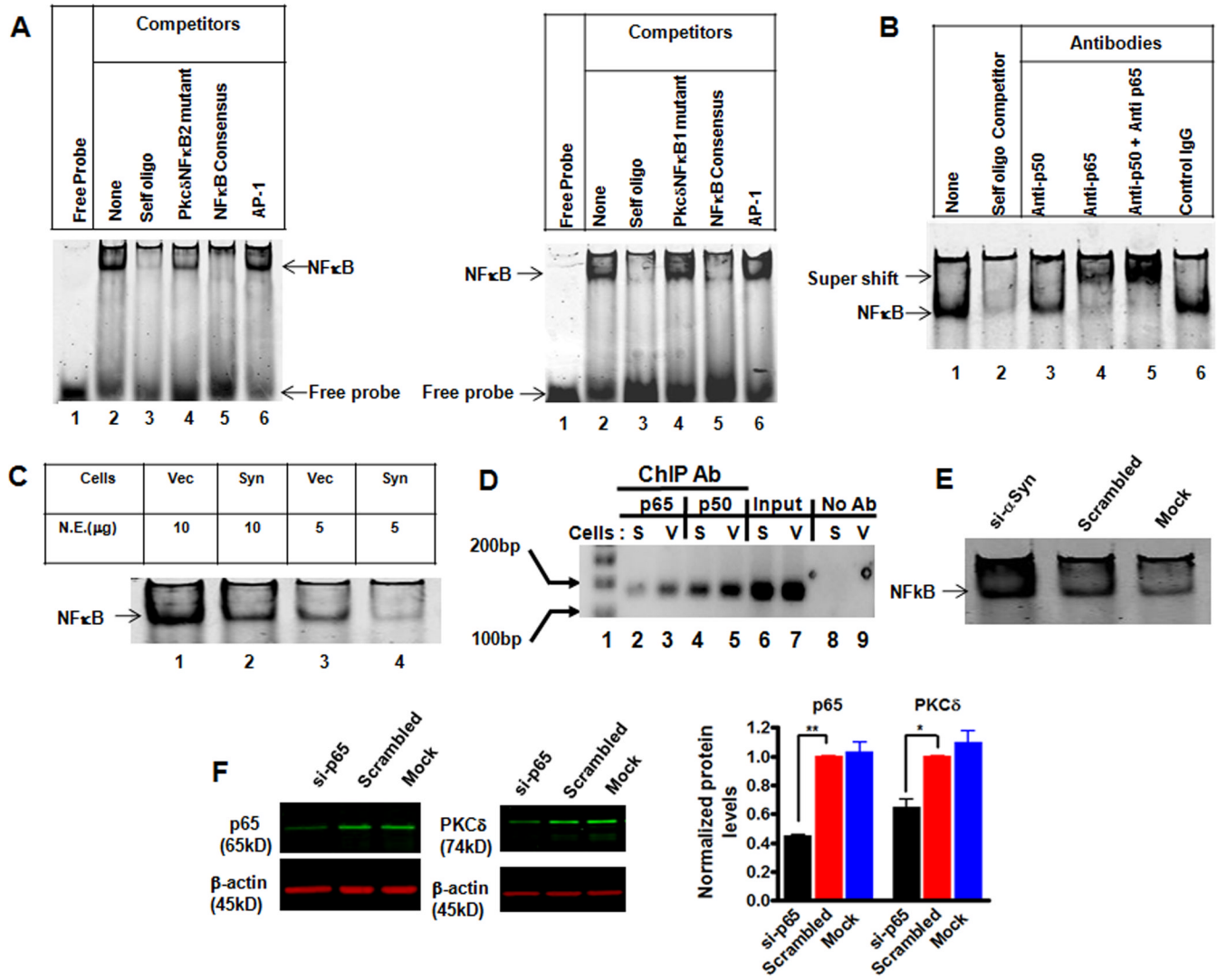

Figure 5.

Increased α-Synuclein expression suppresses PKCδ in part by blocking NFκB activation. ***A***, Representative EMSA gel images show the direct binding of NFκB to the putative PKCδ NFκB sites. Competitive EMSA was conducted using labeled probe corresponding to the PKCδ NFκB site 1 (left panel) or the PKCδ NFκB site 2 (right panel) and indicated unlabeled oligos. ***B***, Binding p50 and p65 to the NFκB sites on the PKCδ promoter. The nuclear extracts from vector control cells were incubated with excess of unlabeled self oligos or indicated antibodies prior to adding the labeled probe (PKCδ NFκB site 1). A representative EMSA supershift gel from three independent experiments is shown. ***C***, A representative EMSA gel image indicates the reduced binding of NFκB *in vitro* to the PKCδ NFκB site 1 in αsyn-expressing N27 cells. ***D***, ChIP analysis of the *in vivo* binding of NFκB-p65 and p50 on the PKCδ promoter. After reversal of cross-linking, immunoprecipitated genomic DNA fragments were analyzed by PCR using primers designed to amplify the −103 to +60 region of PKCδ promoter. ***E***, Knockdown of αsyn protein increased NFκB activity. αSyn-expressing cells were transient transfected with siRNA-αsyn and scrambled siRNA. 72 h post-transfection, the cells were collected and subjected to EMSA analysis using the labeled probe corresponding to the PKCδ NFκB site 1. Mock transfection was also included as a negative control. ***F***, Transfection of NFκB-p65 siRNA down-regulated PKCδ

expression in N27 cells. N27 cells were transfected with p65-siRNA and scrambled siRNA for 96 h, and cells were collected for Western blot analysis. Representative immunoblot (left panel) and quantitation (right panel) of p65 and PKCδ on whole cell lysates in transfected cells. Data are shown as mean ± SEM of two independent experiments (*$p<0.05$, **$p<0.01$).

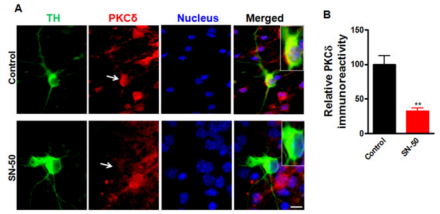

Figure 6.

Effect of NFκB inhibition on the PKCδ immunoreactivity in the primary dopaminergic neurons. ***A***, Primary midbrain cultures were treated with or without 100 μg/ml of SN-50 for 24 h. Cultures were immunostained for TH (green) and PKCδ (red). The nuclei were counterstained by Hoechst 33342 (blue). Images were obtained using a Nikon TE2000 fluorescence microscope (magnification 60×). Scale bar, 10μm. Representative immunofluorescence images are shown. The insert shows a higher magnification of the cell body area. ***B***, Immunofluorescence quantification of PKCδ in TH-positive neurons. Fluorescence immunoreactivity of PKCδ was measured from TH-neurons in each group using Metamorph software. Values expressed as percent of control group are mean ± SEM and representative for results obtained from three separate experiments in triplicate (**$p<0.01$).

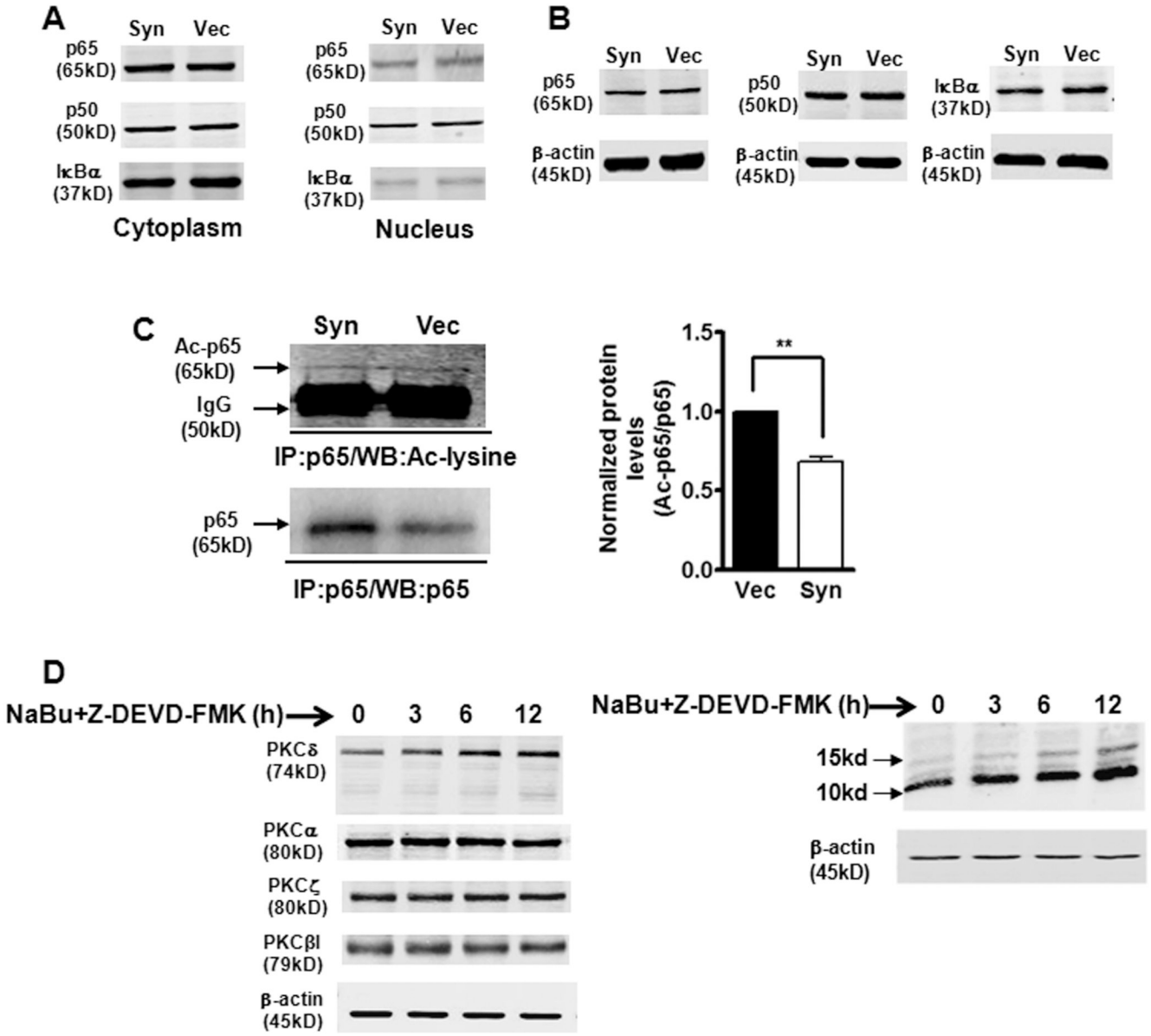

Figure 7.

α-Synuclein-induced blockade of NFκB activation is associated with decreased acetylation of p65, but does not correlate with nuclear translocation or protein levels of NFκB/IκBα. ***A***, ***B***, Nuclear translocation and abundance of NFκB/IκBα were not altered by overexpression of αsyn. Representative immunoblot of p65, p50 and IκBα levels on cytoplasmic and nuclear extracts (*A*) or whole cell lysates (*B*) from αsyn (Syn) and vector control (Vec) cells. ***C***, The p65 acetylation levels were reduced in αsyn cells. Whole cell lysates was immunoprecipitated (IP) with p65 antibody. The resulting immunoprecipitates were blotted with anti-acetyl-lysine and anti-p65 antibodies. Densitometric quantitation of the ratio of band intensity of acetylated p65 and total p65 from two independent experiments (means ± SEM; ***p*<0.01) is shown on the right. ***D***, Sodium butyrate (NaBu) specifically enhanced PKCδ isoform expression in αsyn-expressing N27 cells. αSyn-expressing cells were treated with 1 mM NaBu and 50 μM caspase-3 inhibitor Z-DEVD-FMK, and cell lysates were

prepared for blotting with specific anti-PKC isoforms (left panel) and anti-acetyl-lysine (right panel) antibodies.

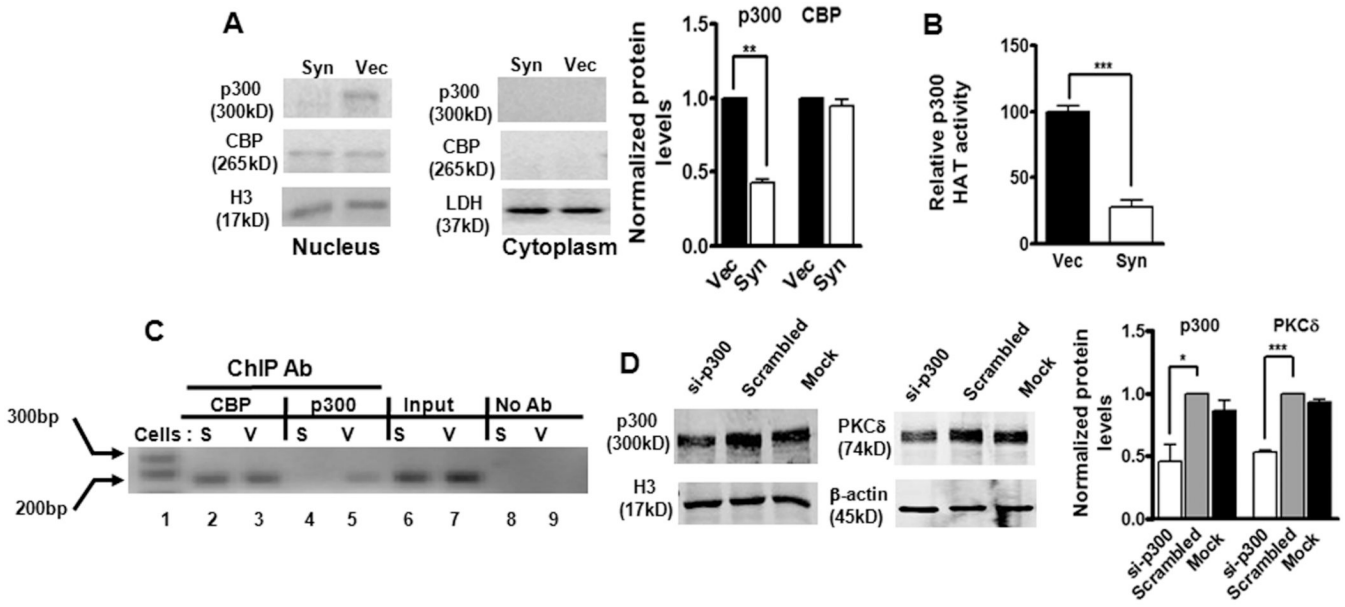

Figure 8.

α-Synuclein down-regulates p300 proteins, resulting in decreased p300 HAT activity and inhibition of p300-dependent transactivation of PKCδ gene expression. ***A***, Decreased p300 protein levels in αsyn-expressing cells. Representative immunoblot (left panel) and quantitation (right panel) of p300 and CBP on cytoplasmic and nuclear extracts from αsyn-expressing (Syn) and vector control (Vec) cells. Data are shown as mean ± SEM of two independent experiments (**$p<0.01$). LDH (cytoplasmic fraction) or histone H3 (nuclear fraction) was used as loading control. ***B***, Decreased p300 HAT activity in αsyn-expressing cells. Data were subtracted from background values that were measured in samples containing normal IgG, and then expressed as the percentage of HAT activity present in vector control cells. Values are shown as mean ± SEM of three independent experiments performed in triplicate (***$p<0.001$). ***C***, The *in vivo* binding of p300 on the PKCδ promoter was interrupted by overexpression of αsyn. After reversal of cross-linking, p300-immunoprecipitated genomic DNA fragments were analyzed by PCR using primers designed to amplify the −103 to +60 region of PKCδ promoter. ***D***, Knockdown of p300 by siRNA-p300 decreased PKCδ levels in N27 cells. N27 cells were transfected with p300-siRNA and scrambled siRNA for 96 h, and cells were collected for Western blot analysis. Representative immunoblot (left panel) and quantitation (right panel) of p300 and PKCδ on nuclear extracts or whole cell lysates in transfected cells. Data are shown as mean ± SEM of two independent experiments (*$p<0.05$, ***$p<0.001$).

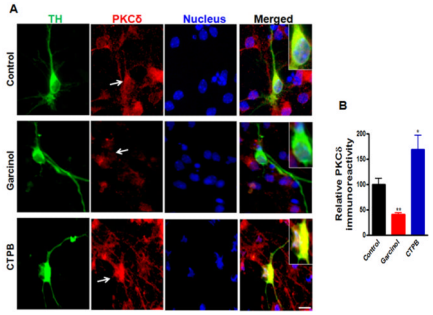

Figure 9.

Effect of p300 inhibition or activation on the PKCδ immunoreactivity in the primary dopaminergic neurons. ***A***, Primary midbrain cultures at 7 DIV were treated with or without either 5 μM garcinol or 10 μM CTPB for 24 h. Cultures were immunostained for TH (green) and PKCδ (red). The nuclei were counterstained by Hoechst 33342 (blue). Images were obtained using a Nikon TE2000 fluorescence microscope (magnification 60×). Scale bar, 10μm. Representative immunofluorescence images are shown. The insert shows a higher magnification of the cell body area. ***B***, Immunofluorescence quantification of PKCδ in TH-positive neurons. Fluorescence immunoreactivity of PKCδ was measured from TH-neurons in each group using Metamorph software. Values expressed as percent of control group are mean ± SEM and representative for results obtained from three separate experiments in triplicate (*$p<0.05$, **$p<0.01$).

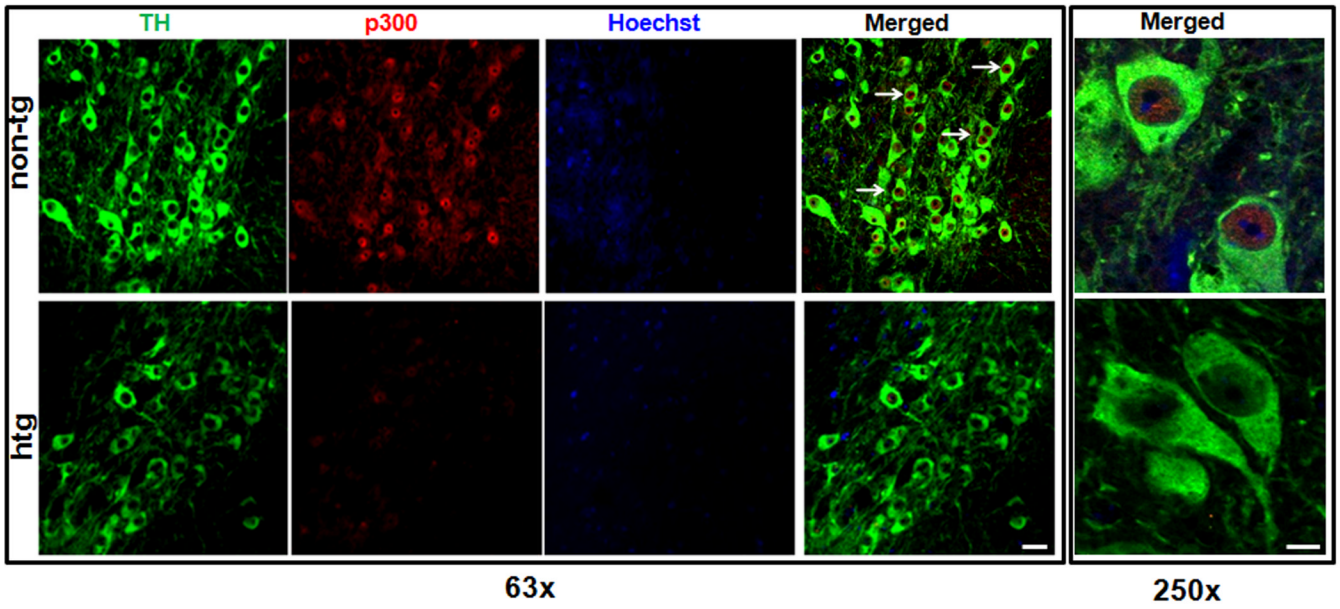

Figure 10.

Decreased p300 level within neurons of the substantia nigra in αsyn overexpressing mice. Representative images of immunohistochemical analysis of p300 expression within nigral TH-positive neurons. Substantia nigra sections from non-transgenic control (non-tg) mice and αsyn transgenic mice (htg) were stained with p300 polyclonal antibody (1:350 dilution) and TH monoclonal antibody (1:1800 dilution), followed by incubation with Alexa 568-conjugated (red; 1:1000) and Alexa 488-conjuated (green; 1:1000) secondary antibodies. Hoechst 33342 (10 μg/ml) was added to stain the nucleus. Confocal images were obtained using a Leica SP5 X confocal microscope system. White arrows point to dopaminergic neurons with significant nuclear p300 staining. Green, TH; red, p300; blue, nucleus. Scale bar, 25μm (left panel) and 7.5μm (right panel). Magnifications 63× (left panel) and 250× (right panel).

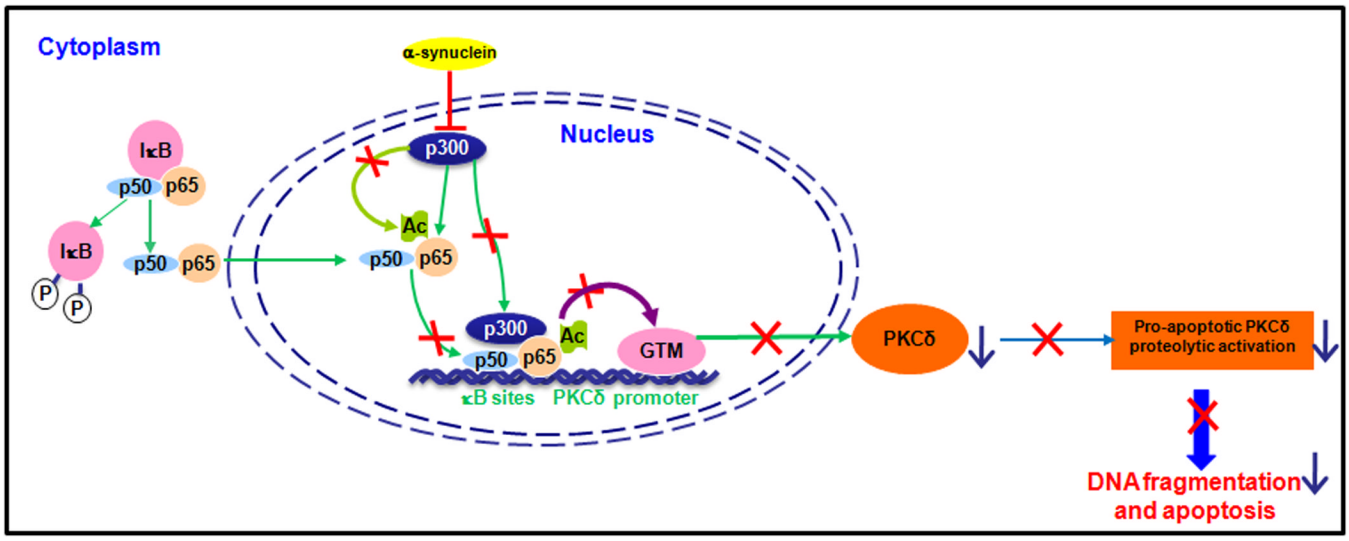

Scheme 1.

A proposed model for α-synuclein acting in the cytoplasm to repress PKCδ expression and attenuate dopaminergic neurotoxicity. Constitutively activated NFκB p50/p65 heterodimers and p300/CBP bind to the two proximal promoter κB sites and modulate PKCδ transcription. Expression of αsyn, a cytoplasmic protein, inhibits p300-mediated acetylation of p65, thereby blocking the NFκB biding to PKCδ promoter. In addition, αsyn reduces p300 protein and its HAT activity, resulting in interruption of binding of p300 to the PKCδ promoter and its interaction with general transcription machinery (GTM), causing inhibition of PKCδ transcription. The resulting loss of PKCδ expression confers protection due to reduced proteolytic activation of PKCδ, which is a key proapoptotic function of the kinase during neurotoxic insults.